Title

Bacteroides fragilis Toxin Coordinates a Pro-carcinogenic Inflammatory Cascade via Targeting of Colonic Epithelial Cells

Journal

Cell Host & Microbe, 23(2)

ISSN

1931-3128

Authors

Chung, Liam
Orberg, Erik Thiele
Geis, Abby L
et al.

Publication Date

2018-02-01

DOI

10.1016/j.chom.2018.01.007

Peer reviewed

HHS Public Access

Author manuscript

Cell Host Microbe. Author manuscript; available in PMC 2018 May 16.

Published in final edited form as:

Cell Host Microbe. 2018 February 14; 23(2): 203–214.e5. doi:10.1016/j.chom.2018.01.007.

BACTEROIDES FRAGILIS TOXIN COORDINATES A PRO-CARCINOGENIC INFLAMMATORY CASCADE VIA TARGETING OF COLONIC EPITHELIAL CELLS

Liam Chung[1,2,3,10], **Erik Thiele Orberg**[2,10,#], **Abby L. Geis**[2,10,#], **June L. Chan**[4], **Kai Fu**[5], **Christina E. DeStefano Shields**[2], **Christine M. Dejea**[6,#], **Payam Fathi**[6,#], **Jie Chen**[4], **Benjamin B. Finard**[1,2], **Ada J. Tam**[1,2], **Florencia M. McAllister**[2,#], **Hongni Fan**[1,2], **Xinqun Wu**[6], **Sudipto Ganguly**[1,2], **Andriana Lebid**[1,2], **Paul Metz**[7], **Sara W. Van Meerbeke**[6], **David L. Huso**[8,&], **Elizabeth C. Wick**[9,#], **Drew M. Pardoll**[1,2], **Fengyi Wan**[2,4,5], **Shaoguang Wu**[6], **Cynthia L. Sears**[1,2,4,6,*], and **Franck Housseau**[1,2,11,*]

[1]Bloomberg-Kimmel Institute for Cancer Immunotherapy, Johns Hopkins University School of Medicine, Baltimore, MD-21287, USA [2]Department of Oncology, Sidney Kimmel Comprehensive Cancer Center at Johns Hopkins University, Baltimore, MD-21287, USA [3]Translational Tissue Engineering Center, Wilmer Eye Institute and Department of Biomedical Engineering, Johns Hopkins University, Baltimore, MD 21287, USA [4]Department of Molecular Microbiology and Immunology, Bloomberg School of Public Health, Johns Hopkins University, Baltimore, MD 21205, USA [5]Department of Biochemistry and Molecular Biology, Bloomberg School of Public Health, Johns Hopkins University, Baltimore, MD 21205, USA [6]Department of Medicine, Johns Hopkins University School of Medicine, Baltimore, MD-21287, USA [7]Department of Pathology, Radboud University Medical Centre, Geert Grooteplein-Zuid 10, 6525 GA, Nijmegen, Netherlands

[*]correspondence: fhousse1@jhmi.edu (F.H) or csears@jhmi.edu (C.L.S.).
[10]these authors contributed equally to the study
[11]Lead contact
[&]deceased
[#]Current addresses: Erik Thiele Orberg, Department of Hematology and Oncology, Klinikum rechts der Isar, Technical University of Munich, Germany; Abby L. Geis, Department of Microbiology & Immunology, Arkansas College of Osteopathic Medicine, Fort Smith, AR 72916, USA; Christine M. Dejea, Center for Drug Evaluation and Research, Food Drug Administration, Silver Spring, MD 20993; Florencia McAllister, Department of Clinical Cancer Prevention. The University of Texas MD Anderson Cancer Center, Houston, TX, USA; Elizabeth C. Wick, Department of Surgery, University of California San Francisco, San Francisco, CA 94143; Payam Fathi, Vanderbilt University School of Medicine, Nashville, TN 37232

DECLARATION OF INTERESTS

The authors declare no competing interests

AUTHOR CONTRIBUTION

C.L.S. and F.H., Supervision
F.H. Project Administration
F.H. and C.L.S., Conceptualization
F.H., C.L.S., L.C. and F.W., Validation
L.C., E.T-O., A.L.G., S.W. and F.W., Methodology
L.C., E.T-O., A.L.G., J.C., K.F., A.J.T., S.W., P.F., B.B.F., H.F., E.C.W., X.W., S.W.V-M., P.M., Investigation
L.C., E.T-O., A.L.G. and K.F., Data Curation
L.C., E.T-O., A.L.G., S.W., D.L.H., Formal Analysis
C.E.D-S., F.M.M., S.G., C.M.D and A.L., Resources
F.H., L.C. and S.W., Visualization
C.L.S., D.M.P., F.W. and F.H. Funding Acquisition
E.T-O., A.L.G. and F.H., Writing-Original Draft
C.L.S. and D.M.P, Writing-Review&Editing

[8]Department of Molecular and Comparative Pathobiology, Johns Hopkins University School of Medicine, Baltimore, MD-21287, USA [9]Department of Surgery, Johns Hopkins University School of Medicine, Baltimore, MD-21287, USA

Summary

Pro-carcinogenic bacteria have the potential to initiate and/or promote colon cancer, in part via immune mechanisms that are incompletely understood. Using Apc^{Min} mice colonized with the human pathobiont enterotoxigenic *Bacteroides fragilis* (ETBF) as a model of microbial-induced colon tumorigenesis, we show that the *Bacteroides fragilis* toxin (BFT) triggers a pro-carcinogenic multi-step inflammatory cascade requiring IL-17R, NF-κB, and Stat3 signaling in colonic epithelial cells (CECs). Although necessary, Stat3 activation in CECs is not sufficient to trigger ETBF colon tumorigenesis. Notably, IL-17-dependent NF-κB activation in CECs induces a proximal to distal mucosal gradient of C-X-C chemokines, including CXCL1 that mediates the recruitment of CXCR2-expressing polymorphonuclear immature myeloid cells with parallel onset of ETBF-mediated distal colon tumorigenesis. Thus, BFT induces a procarcinogenic signaling relay from the CEC to a mucosal Th17 response that results in NFκB activation selectively in distal colon CECs, that collectively triggers myeloid cell-dependent distal colon tumorigenesis.

INTRODUCTION

A microbial etiology of human colorectal cancer (hCRC) has long been proposed and sought (Sears and Garrett, 2014). Establishing how one or more members of the microbiota initiate and/or promote hCRC could stimulate the development of novel prevention approaches, particularly since hCRC has a long lead time from initiation until presentation and at least a subset of putative hCRC microbial drivers are acquired early in life. It has been further proposed that various gut microbes may drive a common pathway to tumorigenesis (Sears and Garrett, 2014). More than 90% of hCRC is sporadic with a small proportion resulting from inherited mutations. Germline mutations in the adenomatous polyposis coli (*APC*) tumor suppressor gene are responsible for Familial Adenomatous Polyposis (FAP), an autosomal dominant disease with a 100% lifetime risk of developing CRC (Kinzler and Vogelstein, 1996). Further, at least 80% of sporadic hCRC also display *APC* mutations. Thus, Apc^{Min} mice that are *Apc* heterozygous ($Apc^{+/-}$) serve as a particularly useful model for hCRC. We have used Apc^{Min} mice colonized with enterotoxigenic *Bacteroides fragilis* (ETBF) as a model of *de novo* microbial-induced colon tumorigenesis, demonstrating that endogenous IL-17 production is tumorigenic and that robust Stat3 activation in immune cells (ICs) and CECs parallels IL-17-dependent colon tumorigenesis (Wick et al., 2014; Wu et al., 2009). Since ETBF colonization is statistically significantly associated with CRC, being detected in ~90% of CRC patients and only ~50% of healthy individuals (Boleij et al., 2015), understanding BFT-mediated epithelial signaling and ETBF oncogenesis is, therefore, proposed as highly relevant to the pathogenesis of human CRC. The key ETBF virulence factor is *Bacteroides fragilis* toxin (BFT), a zinc-dependent metalloprotease that targets, via γ-secretase-dependent signal transduction, epithelial tight junctions through binding to an, as yet, unidentified CEC receptor (Wu et al., 2007; Wu et al., 2006). The epithelial response

to BFT binding induces CEC E-cadherin cleavage resulting in enhanced barrier permeability, Wnt/βcatenin and NFkB signaling in CECs (Wu et al., 1998; Wu et al., 2003; Wu et al., 2004). Similarly, in ETBF-colonized mice, BFT is required for colitis (Rhee et al., 2009). The overt Stat3 activation observed in colons after ETBF colonization is not directly BFT-dependent since, *in vitro*, purified BFT does not induce Stat3 activation in bone marrow-derived dendritic cells (BM-DC) or in HT29 human colon carcinoma cells (Rhee et al., 2009; Wick et al., 2014). Consistent with this idea, Stat3 activation in ETBF-colonized C57BL/6 wild type (WT) mice occurs first in colonic lamina propria (LP) IC, before the detection of a significant increase in colon permeability and CEC Stat3 activation (Wick et al., 2014). Further, initial ETBF-induced Stat3 activation in IC is independent of CEC Stat3 signaling as confirmed in C57BL/6-*Stat3*$^{\Delta IEC}$ mice that lack functional CEC Stat3. Together these results suggest a model by which BFT initiates early, rapid release of epithelial cell mediators that activate Stat3 in a subset of ICs that, in turn, induce IL-17 production and subsequent Stat3 activation in the CEC compartment (Thiele Orberg et al., 2017). However, although similar Stat3 activation occurs from proximal to distal ends of the colon (Wick et al., 2014), ETBF tumorigenesis concentrates in the distal colon. These results suggest that overt CEC Stat3 signaling, alone, does not account for distal colon ETBF tumorigenesis but rather that other epithelial signals collude in distal CECs to promote ETBF tumorigenesis. Most recently, we presented evidence that CEC *Apc* heterozygosity is essential to the accumulation and activation of myeloid derived suppressor cells (MDSC) upon ETBF colonization, again, highlighting that additional intrinsic epithelial signals, yet to be defined, translate the combined action of BFT and IL-17 on CECs to yield a polarized protumoral myeloid environment in the distal colon (Thiele Orberg et al., 2017).

Herein, we establish BFT is the required initiator of a CEC-driven cascade resulting in ETBF-induced distal colon tumorigenesis. Namely, the coordinate action of BFT and IL-17 on *Apc*^{Min} CECs combines with downstream CEC NF-κB activation to stimulate CEC release of CXC chemokines that promote LP accumulation of CXCR2^{+} polymorphonuclear immature myeloid cells (PMN-IMC). Together these elements are required for ETBF-induced distal colon tumorigenesis. Notably, ETBF, through BFT, induces comparable IL-17 and Stat3 activation along the length of the colon but enhanced distal colon CEC NF-κB activation. Thus, distal CEC NF-κB activation is a strategic coordinator for the protumoral contributions of the BFT, IL-17 and Stat3. Further, Stat3 activation in ICs and CECs occurs upon ETBF colonization independently of both IL-17R signaling and IL-6 production, two factors commonly invoked as critical in other colon tumorigenesis models (Grivennikov et al., 2009; Grivennikov et al., 2012; Wang et al., 2009). Our data emphasize that BFT action on CECs colludes with three major mucosal proinflammatory signaling pathways, NFκB, Stat3 and IL-17R, all strictly required for ETBF tumorigenesis in Min mice and all closely associated with CRC in human (De Simone et al., 2015; Wang et al., 2014; Wu et al., 2009). Our findings support the potential utility of identifying pharmacological agents, such as CXCR2 inhibitors, to reprogram the immune microenvironment and disrupt downstream stages of bacterial-induced carcinogenesis while preserving microbiota and beneficial IL-17-dependent anti-microbial mechanisms (Chen et al., 2016; Conti et al., 2016; Kumar et al., 2016).

RESULTS

BFT and epithelial-expressed IL-17R are required for ETBF-triggered tumorigenesis

We first colonized *Apc*^{Min} mice with an ETBF strain possessing an in-frame chromosomal deletion of *bft* [ETBF(*Δbft*)] to test the contribution of BFT to ETBF tumorigenesis. Whereas *Apc*^{Min} mice colonized with the parental ETBF strain developed an average 18.5±5.2 colon tumors 3 months after colonization, tumor numbers were indistinguishable between sham and ETBF(*Δbft*)-colonized *Apc*^{Min} mice (1.8±0.5 versus 1.7±0.8; Fig 1A) indicating BFT is required for ETBF tumorigenesis. ETBF tumors are commonly adenomas leading to bowel obstruction and murine death in 3 months or less after ETBF colonization prior to carcinomatous transformation. Next, we sought to better understand the role of IL-17 in promoting colon tumorigenesis during ETBF colonization of *Apc*^{Min} mice (Wu et al., 2009). *Il17a*$^{-/-}$ and *Il17ra*$^{-/-}$ *Apc*^{Min} mice were significantly resistant to ETBF-mediated tumorigenesis (5.2±1.3 and 3.8±0.8 colon tumors, respectively, *versus* 15.8±2.7 in parental *Apc*^{Min} mice, p<0.0001; Fig. 1B). Thus, we confirmed previous *in vivo* antibody-blockade studies showing that IL-17 is a key pro-inflammatory mediator promoting tumor formation in ETBF-colonized *Apc*^{Min} mice (Wu et al., 2009). IL-17R can mediate its carcinogenic effect either directly on IL-17R^{+} CEC or by acting on other target IL-17R^{+} cell types, including tumor-associated fibroblasts (TAF), macrophages (TAM) or MDSC, with production of mediators that, in turn, promote epithelial tumor growth (Iwakura et al., 2011). Therefore, to determine whether IL-17 acted on mucosal leukocytes or CECs to yield ETBF tumorigenesis, we generated bone marrow (BM) chimera *Apc*^{Min} mice, using lethally irradiated parental *Apc*^{Min} mice reconstituted with *Il17ra*$^{-/-}$ BM ([*Il17ra*$^{-/-}$> *Apc*^{Min}]) and, conversely, *Il17ra*$^{-/-}$ *Apc*^{Min} mice reconstituted with wild type C57BL/6 (WT) BM ([WT>*Il17ra*$^{-/-}$ *Apc*^{Min}]). *Apc*^{Min} mice reconstituted with WT BM [WT> *Apc*^{Min}] served as a positive control cohort to evaluate tumorigenesis 3 months after ETBF colonization. We found that [*Il17ra*$^{-/-}$> *Apc*^{Min}] and [WT>*Apc*^{Min}] mice yielded similar tumor numbers (16.5±3.7 *versus* 16.7±3.5; p=0.98, Fig 1C) whereas the absence of non-hematopoietic IL-17R in the recipient *Apc*^{Min} mice [WT>*Il17ra*$^{-/-}$-*Apc*^{Min}] nearly ablated ETBF tumorigenesis (0.6±0.4 *versus* 22.9±3.6 in [WT>*Apc*^{Min}], p=0.0003, Fig. 1D). We recently published that IL-17 produced by Th17 and γδT17 is responsible for ETBF-driven colon tumorigenesis (Housseau et al., 2016). Thus, together, these results suggest that ETBF-induced T cell-derived IL-17 mediates its tumor-promoting effects mainly *via* its activity on IL-17R-expressing non-hematopoietic-derived cells. To further define IL-17R expression in our murine model, we examined the tissue distribution of IL-17R by immunofluorescence (IF) using formalin-fixed paraffin embedded (FFPE) colon tissue sections obtained from ETBF-colonized *Apc*^{Min} mice. Fig. 1E shows that expression of IL-17R was dominant in CECs. Notably, tumorigenic CECs present in microadenomas retained high level IL-17R expression. Combined with our prior data indicating that only the CEC *Apc* mutation is required to initiate ETBF colon tumorigenesis (Thiele Orberg et al., 2017), we next focused on analyzing IL-17-mediated signaling in the epithelial compartment to better understand the BFT/IL-17 cooperation in triggering colon tumorigenesis.

Higher IL-17-dependent NF-κB activation in distal colon CECs parallels the regional distribution of ETBF-induced tumors

The mechanism(s) driving the marked distal localization for colon tumorigenesis is unknown. Thus, to understand the CEC-associated molecular mechanisms involved in IL-17-dependent ETBF distal colon tumorigenesis, we first compared the expression of inflammation-related (Ir) genes in CECs isolated from ETBF-colonized WT *versus Il17*$^{-/-}$ C57BL/6 mice. Colons were divided into 6 juxtaposed sections from distal (C1) to proximal end (C6; Fig. 2A). CD45^{-}EpCAM^{+} CECs were cell-sorted from the distal C1+C2 colon sections ($DC_{1–2}$) of 7 day-colonized WT mice instead of *Apc*^{Min} mice in order to exclude interference by early ETBF tumorigenesis and *Apc* mutation-augmented Wnt signaling on NF-κB activation. CECs expressed *Defb2* (encoding Defensin β2), *Cxcl12* (encoding SDF-1), *Cxcl1* (encoding KC), *Ptgs2* (encoding COX2), and *Reg3b* at a higher level when isolated from the distal colon of WT mice compared to *Il17*$^{-/-}$ mice 7 days after ETBF colonization (Fig. S1). Our observations that ETBF-induced CEC expression of the IL-17 target genes encoding KC (*Cxcl1*) and SDF-1 (*Cxcl12*), critical chemokines for leukocyte trafficking, led us next to test the hypothesis that ETBF colonization induced a distal colon gradient of IL-17 potentially underlying the regional ETBF inflammatory and tumor effects. We used Taqman-based qRT-PCR to measure the expression of *Il17a* and IL-17-target genes, *Cxcl1, Cxcl2* and *Cxcl5,* in each of six colon sections after 7 days of ETBF colonization (Fig. 2). Strikingly, while gradients of *Il17a, Il17ra* and/or *Il17rc* mRNA were not detected along the colon axis, there was a pronounced gradient of *Cxcl1*, *Cxcl2* and *Cxcl5* mRNA expression that increased from the proximal to distal colon (Fig. 2A). Chemokine gene expression was abrogated in *Il17*$^{-/-}$ and *Il17ra*$^{-/-}$mice demonstrating that IL-17 triggered the CXC chemokine production (Fig. 2A). We confirmed in 7 day-colonized C57BL/6 mice that the chemokine gradient was induced in the CEC fraction by assessing the gene expression selectively in CECs isolated from the successive colon sections from the proximal to distal colon (Fig. S2A). We further evaluated whether ETBF preferentially colonizes the mucosa of the distal colon of *Apc*^{Min} mice to drive the preferential colon tumorigenesis in the distal region. Paradoxically, we found that ETBF mucosal adherence along the colon axis was significantly less in the distal versus proximal colon of *Apc*^{Min} mice (p=0.008; Fig. S2B). In contrast, ETBF mucosal adherence was similar in the proximal and distal colon of IL-17$^{-/-}$ and IL-17R$^{-/-}$ *Apc*^{Min} mice (Fig. S2B). These results demonstrated that increased distal colon *Apc*^{Min} mouse ETBF colonization does not drive ETBF colon tumor localization; conversely, reduced ETBF colonization does not underlie the decreased tumorigenesis in *Apc*^{Min} mice deficient in IL-17 CEC signaling. Nevertheless, BFT secretion by ETBF is required to generate the gradient of *Cxcl1*, *Cxcl2* and *Cxcl5* gene expression as the gradients of chemokine gene expression are lost in mice colonized with the ETBF(*Δbft*) strain (Fig. S2). Similar to the *Il17ra* and *Il17rc* mRNA levels, the IL-17R protein level in CEC was largely comparable along the colon axis upon ETBF colonization (Fig. 2B), indicating that the elevated C-X-C chemokine gene expression in the distal colon of ETBF-colonized mice most likely does not result from enhanced IL-17R expression. We did not find significant ETBF-mediated changes in expression of either *Tnfaip3* that encodes the deubiquitinase, A20, a negative regulator of IL-17R (Garg et al., 2013) or *Elavl1* encoding the protein Hur (Herjan et al., 2013) that is involved in in Act1-mediated stabilization of Cxcl mRNA upon IL-17 signaling (Fig. S2). These results suggested that

increased expression of the inflammatory cytokines along the colon axis is not due to regulatory feedback on epithelial IL-17R signaling or mRNA stabilization. Since C-X-C chemokines are known to be tightly regulated by NF-κB and Stat3 transcription factors, we tested the activation of NF-κB and Stat3 along the colon axis, by immunoblotting for the nuclear translocation of p65 and pStat3, respectively, in the CECs derived from ETBF-colonized and sham colons. The nuclear pStat3 levels were comparable along the colon (Fig. 2B), consistent with our previously reported IHC staining results (Wick et al., 2014). In contrast, the nuclear translocation of p65 was substantially enhanced in the CECs isolated from middle (M; C3+C4) and distal (D; C1+C2) colon sections *versus* proximal (P; C5+C6) section of ETBF-colonized colons compared to sham colons (Fig. 2B), suggesting that ETBF colonization triggers more robust NF-κB signaling in the distal colon. Moreover, p65 nuclear accumulation in the ETBF-colonized M and D colon sections was diminished when *Il17ra*$^{CEC-/-}$ mice were used (Fig. 2C), demonstrating that the ETBF-induced NF-κB activation is IL-17R dependent. In support of this notion, we observed that BFT and IL-17 each directly induced p65 nuclear translocation in the BFT-sensitive human colon carcinoma cell line, HT29/C1 (Fig. 2D). In contrast, neither BFT nor IL-17 directly induces Stat3 activation in HT29/C1 cells (Wick et al., 2014). Finally, we confirmed the functional relevance of BFT and IL-17-initiated NF-κB activation by determining that both significantly increased IL-8 (human homologue to murine CXCL1/KC) secretion by HT29/C1 cells after a 4 hour-treatment. (Fig. S3). Altogether, our findings suggest that ETBF colonization, *via* BFT, initiates selective distal colon NF-κB activation, dependent on IL-17 and the CEC IL-17R that results in a gradient of C-X-C chemokine production. This BFT/IL-17:IL-17R/NF-κB distal colon cascade correlates with the distal localization of ETBF-induced colon tumors (Wu et al., 2009).

IL-17 induces myeloid cell accumulation and tumorigenesis in the distal colon of ETBF-colonized mice *via* CXCR2-dependent mechanism(s)

Loss of IL-17 production or IL-17R signaling in CECs reduces ETBF colon tumorigenesis (Fig. 1B&D) and impacts the expression of chemokines (CXCL1, CXCL2, CXCL5 and CXCL12) that recruit myeloid cells (Fig. S1 and Fig. 2) Thus, we tested the hypothesis that the response of CECs to IL-17 dictates the geographic distribution of myeloid populations in the colonic lamina propria (LP), allowing their preferential trafficking to the distal portion of the colon. Consistent with this hypothesis, ETBF colonization induced an accumulation of polymorphonuclear (PMN) immature myeloid cell (IMC) (CD11b^{hi}Ly6G^{pos}Ly6C^{int})] in distal colon (defined as C1+C2; DC_{1-2}) when compared to sham DC_{1-2} (355±122 versus 5±2 cells/mg tissue, respectively, p=0.002; Fig 3A) or compared to proximal-middle (PM) colon (defined as C4+C5; PMC_{4-5}) 7 days after ETBF colonization (355±122 versus 36±9 cells/mg tissue, respectively, p=0.0134; Fig. 3B). Although increased, the proportion of monocytic (MO)-IMC (CD11b^{hi}Ly6C^{hi}Ly6G^{neg}) in the distal colon was not significantly different from P-M colon upon ETBF colonization. The PMN-IMC recruitment to the distal colon was impaired in *Il17a*$^{-/-}$ mice confirming the role of IL-17 in promoting the trafficking of PMN-IMC cells (18,611±860 PMN-IMC per DC in WT versus 2,470±966 per DC in Il17$^{-/-}$ mice, p=0.021; Fig. 3C). In contrast, IL-17 loss did not significantly impact monocytic (MO)-IMC (13,471±5,162 MO-IMC per DC in WT versus 2,848±1,371 in *Il17a*$^{-/-}$ mice, p=0.116) or tissue resident macrophage (Mϕ) accumulation [MHCII^{hi}-Mϕ (CD11b

$^{+}$Ly6C^{neg}Ly6G^{neg}F480^{pos}I-A/E^{hi}; 15,740±2,804 per DC versus 12,514±3,800, p=0.503) and MHCII^{lo}-Mϕ (CD11b^{+}Ly6C^{neg}Ly6G^{neg}F480^{pos}I-A/Elo; 19,056±6,773 per DC versus 6,799±2,383, p=0.150) (Fig. 3C). We previously showed that MO- and PMN-IMC recruited in colonic tissue upon ETBF-triggered colitis are MDSCs (Thiele Orberg et al., 2017).

In CXCR2$^{-/-}$ mice (CXCR2 being the receptor for CXCL1, CXCL2 and CXCL5), PMN-IMCs were significantly reduced in the distal colon 7 days after ETBF colonization compared to WT mice (PMN-IMC, 5,810±4,631 per DC in CXCR2$^{-/-}$ mice versus 20,412±4,739 in WT mice, p=0.0474; Fig. 4A). Importantly, in CXCR2$^{-/-}$ mice, IL-17-producing cells were still present in colon tissue, confirming that IL-17-mediated signaling is upstream of NF-κB activation and C-X-C chemokine (i.e. CXCL1, CXCL2 and CXCL5) production by CECs (Fig. 4B). Because CXCR2 is mainly expressed by myeloid cells and, more specifically, PMN leukocytes (Fig. S4), we further tested the impact of impaired myeloid trafficking on ETBF-triggered colon tumorigenesis using lethally irradiated *Apc*^{Min} mice reconstituted with BM from CXCR2$^{-/-}$ *versus* CXCR2$^{+/+}$ (WT) mice ([CXCR2$^{-/-}$>*Apc*^{Min}] and [WT>*Apc*^{Min}], respectively). We found that, upon ETBF colonization, [CXCR2$^{-/-}$>*Apc*^{Min}] mice exhibited reduced colon tumorigenesis compared to control [WT>*Apc*^{Min}] mice (Fig 4C, 10±2.7 versus 21±4.9, respectively, p=0.04). Although the expression of another IL-17 target gene *Cxcl12* (encoding SDF-1) was dramatically decreased in *IL17a*$^{-/-}$ compared to *IL17a*$^{+/+}$ WT distal CECs (Fig. S1), mice deficient for *Cxcr4* (coding CXCL12/SDF-1 receptor) expression in myeloid cells (CXCR4$^{\Delta lysm}$-*Apc*^{Min}) did not exhibit decreased numbers of tumors. Similarly, $CX_3CR1^{-/-}$ (the receptor of CX_3CL1/fractalkine involved in LP macrophage trafficking) and IL6Ra$^{\Delta lysm}$ *Apc*^{Min} mice, did not display reduced tumor numbers (Fig. S5). Together these results point to the specificity of a CXCR2-dependent myeloid recruitment, and therefore PMN cells, to colon tumorigenesis following ETBF colonization. We next used pepducin, a peptide that uncouples CXCR2 ligand binding from its signaling transduction adaptor (Jamieson et al., 2012), to further test the contribution of CXCR2 to ETBF myeloid recruitment and tumorigenesis. Pepducin treatment diminished ETBF-induced myeloid cell recruitment, especially PMN-IMC ((24,300±3,412 PMN-IMC per DC in control versus 9,707±1,973 in pepducin-treated mice, p=0.0031, Fig 4D), as also observed in Cxcr2$^{-/-}$ mice. The decrease of PMN-IMC in distal colon did not significantly impact the colonic mucosa expression of *Il17a*, *Cxcl1*, *Cxcl2* and *Cxcl5* genes expression, demonstrating again that IL17-mediated CEC activation is upstream of CXCR2-dependent myeloid trafficking (Fig. 4E). Whereas activated myeloid cells are an important mucosal source of IL-23 stabilizing the Th17 lineage (Grivennikov et al., 2012), paradoxically, we found that ETBF-colonized IL-23p19$^{-/-}$ *Apc*^{Min} mice retained LP IL-17 production and colon tumorigenesis (Fig. S6). Altogether, these results suggest that the decrease of tumor numbers in Cxcr2$^{-/-}$ Apc^{Min} mice is likely not related to a deficit in myeloid-derived IL-23. Lastly, consistent with our hypothesis that distal colon myeloid recruitment is required for ETBF tumorigenesis, daily pepducin administration to ETBF-colonized *Apc*^{Min} mice resulted in significantly lower numbers of microadenomas at 4 weeks-post colonization compared to *Apc*^{Min} mice treated with a control peptide (1.2±0.3 *versus* 2.2±0.4; p=0.0214; Fig. 4F).

Epithelial Stat3 signaling is required for ETBF-triggered tumorigenesis, but is not dependent on IL-17, IL-6 nor myeloid cells

Based on chemically-induced cancer models, dysregulation of the proinflammatory NF-κB/IL-6/Stat3 cascade is commonly hypothesized as being critical to tumor proliferation and survival (Bollrath et al., 2009; Grivennikov et al., 2009; Yu et al., 2009). To test this theory in our bacterial-induced colon tumorigenesis model, we used *Apc*^{Min} mice with deficiency in Stat3 signaling selectively in myeloid (Stat3$^{\Delta lysm}$-*Apc*^{Min}) or, alternatively, in the epithelial compartment (Stat3$^{\Delta IEC}$-*Apc*^{Min}). Stat3 deficiency in the myeloid compartment did not decrease ETBF tumor numbers (data not shown). In contrast, epithelial Stat3 deficiency nearly ablated ETBF tumor development (12.4±3 in *Apc*^{Min} mice *versus* 3.8±0.9 in Stat3$^{\Delta IEC}$-*Apc*^{Min} mice, p=0.005; Fig. 5A) but did not impair MO- or PMN-IMC trafficking (18,489±6,000 per DC *versus* 16,988±6,900, p=0.876 and 11,105±3,371 per DC *versus* 12,272±4,683, p=0,900, respectively) to the distal colon, although Mϕ-MHC-II^{lo} were significantly increased in mice deficient in epithelial Stat3 signaling (16,719±4465 per DC in WT versus 56,985±14,196 in Stat3$^{\Delta IEC}$ mice, p=0.0167; Fig. 5B). Further, ETBF mucosal adherence did not differ in the proximal and distal colon of Stat3$^{\Delta IEC}$-*Apc*^{Min} mice (Fig. S2B). Remarkably, colon tumorigenesis decreased without significant loss of IL-17-producing LP cells (9,099±3,838 per DC in WT *versus* 4,498±2,497 in Stat3$^{\Delta IEC}$-*Apc*^{Min} p=0.363 for Th17 cells and 15,578±6,437 per DC in WT *versus* 9,512±4,106 in Stat3$^{\Delta IEC}$-*Apc*^{Min} p=0.175 for total IL-17-producing cells) or global *Il17a* expression (172.2±139.6 per DC in WT *versus* 119.4±62.4, p=0.469) in colonic mucosa showing that, although critical to colon tumorigenesis, epithelial Stat3 activation is not a critical contributor to Th17 nor γδT17 cell differentiation or total mucosal IL-17 upon ETBF colonization (Fig. 5C&D).

Stat3 activation is regulated by a wide array of cytokines and growth factors, yielding pleiotrophic cellular effects (Yu et al., 2009). In CECS, Stat3 activation by IL-6, IL-10/IL-22 and IL-23 has been shown to facilitate oncogenesis (Bollrath et al., 2009; Grivennikov et al., 2009; Grivennikov et al., 2012; Kryczek et al., 2014). Since IL-6, produced by myeloid and potentially other cells, is proposed as a key protumoral mediator activating Stat3 in its target cells (Bollrath et al., 2009), we tested whether IL-6 production in the TME as well as epithelial IL-6R contributes to epithelial Stat3 activation and tumor development upon ETBF colonization of *Apc*^{Min} mice. Surprisingly, we found no significant decrease of tumor numbers in IEC$^{\Delta Il6ra}$ (Fig. S5) and only a non-significant trend in *Il6*$^{-/-}$ *Apc*^{Min} compared to parental *Apc*^{Min} mice colonized with ETBF (18.7±3.7 in *Apc*^{Min} versus 10.8±1.9 in *Apc*^{Min}-*Il6*$^{-/-}$ mice, p=0.354; Fig. 5E), suggesting a non-essential role for IL-6 in ETBF-induced colon carcinogenesis. We further determined that, although IL-6 was necessary for Th17 and ILC3 differentiation, γδT17 cells were unaltered in the LP (Fig. S7A and B). The resulting decrease of total IL-17-producing cells in LP of *Il6*$^{-/-}$ mice 7 days after ETBF colonization (Fig. S7B) only led to a moderate and non-significant decrease in *Il17a* mRNA expression (Fig. 5F). Because of the discrepancy in tumor number reduction between the IL-6$^{-/-}$- and Stat3$^{\Delta IEC}$-*Apc*^{Min} mice, we, then, sought to better understand the mechanism of Stat3 activation in ETBF-colonized mice and performed pStat3 IHC on colons collected from *Apc*^{Min}, *Il17a*$^{-/-}$ *Apc*^{Min}, *Il6*$^{-/-}$ *Apc*^{Min}, [*Cxcr2*$^{-/-}$ BM >*Apc*^{Min}] and [WT BM >*Apc*^{Min}] mice 3 months after ETBF colonization (Fig. 6). Surprisingly, epithelial Stat3 activation (pStat3 staining) was still strongly detected in CEC and immune cells in all

cases. Given the role of IL-22-induced Stat3 activation in epithelial cells to promote regeneration following tissue damage (Lindemans et al., 2015), we also tested epithelial expression of *Il22, Il22ra, Il20* and *Il24* RNA along the colon (Fig. S2). No gradient of *Il22ra* expression between the proximal and distal end of the colon was identified. Consistent with our detection of low expression of *Il22* and *Il24* in the distal portion of ETBF-colonized colons, we found that Stat3 activation by IHC in *Il22*$^{-/-}$ *Apc*^{Min} mice 3 months after ETBF colonization was similar to that detected in parental *Apc*^{Min} mice (Fig. 6B). Together our data highlight that, in our ETBF model, Stat3 activation is likely due to a combination of activators with the IL-22 axis playing a minor role. Nonetheless, Stat3 activation in CECs (Fig. 5A), together with BFT, IL-17 (Fig. 1) and myeloid recruitment (Fig. 4), are required for ETBF tumorigenesis.

Discussion

In our model of *de novo* ETBF-induced tumorigenesis, we previously established that IL-17 is required for colon tumor development in colonized *Apc*^{Min} mice (Housseau et al., 2016; Wu et al., 2009). Upon ETBF colonization, the colonic epithelium is characterized by rapid Stat3 activation in ICs and then in CECs (Wick et al., 2014), but a deeper understanding of the pathogenesis of ETBF-induced tumor formation and the mechanistic relationship between BFT-mediated CEC action and IL-17 signaling pathways in CECs during ETBF tumorigenesis has yet to be established.

We previously showed that BFT binds directly to an epithelial receptor, yet to be identified, to mediate E-cadherin cleavage and onset of colitis (Wu et al., 2006). Although, in the absence of an identified BFT receptor, the downstream signaling pathway(s) stemming from BFT CEC binding remain unclear, our findings herein establish the strict combined requirement for CEC IL-17R and Stat3 signaling pathways to sustain BFT-dependent colon tumorigenesis in ETBF-colonized *Apc*^{Min} mice. Remarkably, in the absence of any one of these components, ETBF-triggered tumorigenesis is almost entirely abrogated. IL-17R signaling in CECs does not activate Stat3 but rather activates NF-κB that, in turn, induces key chemokines, including CXCL1, yielding pro-tumoral IMC/MDSC recruitment in a CXCR2-dependent fashion. Stat3 and NF-kB are two core transcriptional factors regulating inflammatory signaling pathways that are intimately linked to the tumor-associated inflammatory environment (Yu et al., 2009). Further, we show that IL-17 did not exert its dominant pro-tumoral role through its control on production of the NF-kB-dependent mediator, IL-6, (Wang et al., 2014; Wang et al., 2009) since the deletion of IL-6 or epithelial IL-6R did not impair CEC Stat3 activation and only non-significantly decreased colon tumor numbers upon ETBF colonization. Interestingly, we found that not only IL-6, but also IL-23 (Fig. S6&S7), is dispensable to ETBF-triggered IL-17 production in the colon, a result that calls into question the obligate IL-6-driven Stat3 and IL-23-dependent Th17 pathways proposed for microbial-induced colon tumorigenesis (Grivennikov et al., 2009; Grivennikov et al., 2012). The IL-23/IL-17 axis along with myeloid cell activation associated with epithelial barrier impairment (Grivennikov et al., 2012) is seemingly not critical during ETBF tumorigenesis. Our findings confirm the functional redundancy of Th17 and γδT17 cells (Housseau et al., 2016), since Th17 cells persist in the absence of Il-23 (Fig. S6) and γδT17 cells in the absence of IL-6 (Fig. S7); the γδT17-produced IL-17 is sufficient to

sustain ETBF-triggered colon tumorigenesis independently of IL-6 and IL-23 (Housseau et al., 2016).

The notable regional localization of ETBF tumorigenesis to the distal murine colon is a highly consistent feature of this model (Wu et al., 2009). While the number of colon tumors triggered by ETBF colonization of Apc^{Min} mice varies, these tumors cluster in the distal colon and only rarely are identified in the proximal mouse colon. Our data indicate that ETBF colon tumorigenesis absolutely requires BFT along with the subsequent cooperation of the IL-17R and Stat3 signaling pathways. This ETBF tumorigenesis initiation appears nucleated around an increased distal CEC NF-kB response to BFT because we did not identify contributing differences in the mucosal abundance of ETBF, expression of IL17/IL17R or Stat3 activation between the proximal and distal colon Of note, however, the activation of NF-kB and expression of its target genes *Cxcl1*, *Cxcl2* and *Cxcl5* were increased in the distal colon, coinciding with the preferential distribution of tumors. As we sought to resolve the sequence of events resulting in the distal distribution of ETBF tumors, we tested a model in which NF-kB-mediated CEC response to IL-17 and/or BFT drives the recruitment of protumoral myeloid cells in the distal colon that likely promote tumor growth (Fig. 7). We recently established that the immune microenvironment of ETBF colon tumors displays a myeloid immune signature including the $iNOS^{hi}$ MO-MDSC and a predominant population of PMN-MDSC, a protumoral inflammatory environment that differs strikingly from that associated with *Fusobacterium nucleatum* and *pks+E. coli* colonization (Thiele Orberg et al., 2017), two additional bacteria linked to CRC in humans and shown to induce colon tumorigenesis in experimental murine models (Sears and Garrett, 2014). High IL-17 levels in combination with MDSCs (including $iNOS^{hi}$ MO-MDSC) accumulated in the distal colon selectively marked the pathogenic interaction of ETBF with colon CECs (Thiele Orberg et al., 2017). Yet, we did not understand the relative roles played by both MDSC populations in the ETBF tumorigenesis process. Using *Cxcr2* deletion or CXCR2 signaling inhibition via pepducin treatment, we found herein that impaired trafficking of the PMN-, and to lesser extend MO-IMCs (likely MDSCs; see Thiele Orberg et al. 2016), to the distal colon decreased tumorigenesis without compromising mucosal IL-17 production or epithelial Stat3 activation. These results establish that the myeloid environment shaped by the upstream epithelial IL-17R/NF-kB activation following initial BFT action, fosters the regional distribution of ETBF colon tumors. Notably, the geographic distribution of the myeloid IMCs/MDSCs following ETBF colonization, essentially distal, did not match the overall Stat3 activation in colonic epithelium, a feature that counters the idea that the selective distal accumulation of IMCs/MDSCs observed is primarily responsible for CEC STAT3 activation and subsequent tumorigenesis. The distal clustering of IMCs/MDSCs likely provides critical factors promoting distal colon tumor growth but we cannot exclude that other myeloid cell subsets, including Mϕ (Fig. 5B) that do not express CXCR2 (Fig. S4), may also deliver Stat3-activating mediators along the ETBF-colonized colon epithelium.

Importantly, the fact that pStat3 in the proximal colon after ETBF colonization is not associated at later time points with microadenoma formation and tumor development (Wick et al., 2014; Wu et al., 2009), even in the presence of IL-17 and BFT, supports a critical role for additional intrinsic distal CEC components, not yet fully identified, in the regional

distribution of colon tumorigenesis. Herein, we identified that ETBF adherence to the murine colon epithelium triggers a distinct response between proximal and distal colon, featuring NF-kB activation. (Wu et al., 2006). It is reasonable to propose that the epithelial response (NF-kB signaling) to ETBF colonization might also be conditioned by the expression of the putative CEC-associated receptor to BFT (Wu et al., 2006). Nevertheless, awaiting for the identification of BFT receptor, our results emphasize that, although critical to ETBF tumorigenesis, Stat3 activation alone is not a marker for tumor development in the ETBF-colonized murine colon

Since IL-6 is dispensable for promoting either tumorigenesis or Stat3 activation in ETBF-colonized mice, it will be critical to understand the nature of the mediator(s) provided by the myeloid environment, and especially PMN-MDSCs, that promote tumorigenesis. Recently, the group of J. Massagué showed that myeloid $CD11b^{+}GR1^{+}$ cells, trafficking via the production of a CXCL1 gradient provided by breast epithelial cells, secrete the inflammatory mediator, S100A8/9, that enhanced breast cancer cell survival without involving Stat3 activation (Acharyya et al., 2012). Interestingly, we previously described the production of high level S100A8/9 by colonic MDSCs recruited upon ETBF colonization and independent of IL-17R expression by this myeloid population (Thiele Orberg et al., 2017). From a translational viewpoint, the association of ETBF with hCRC (Boleij et al., 2015) and our results herein suggest that identification of pharmacological targets aimed at countering the procarcinogenic properties of ETBF may disrupt hCRC development such as by selectively neutralizing the deleterious inflammatory consequences of ETBF colonization. Similarly, the potential for clinical application of the finding that CXCR2 antagonists counter ETBF colon tumorigenesis is of high interest since these agents impair the trafficking of MDSCs without blocking the protective antibacterial properties of IL-17 during acute infection that, in general, contribute to the eradication of colon microbial pathogens. In our hands, the blockade of IL-17A or the use of IL-17/IL-17R KO mice impaired mucosal defenses and was associated with excess mortality upon ETBF colonization (not shown), making IL-17 likely a poor target for inhibition in the colon. By breaking the negative feedback loop between MDSCs and IL-17-stimulated Apc^{Min} CECs during ETBF colitis, it is possible that CXCR2 inhibitors could block protumoral MDSC recruitment, increase Th17 mucosal anti-bacterial responses, and facilitate the eradication of ETBF without promoting tumorigenesis.

STAR METHODS

CONTACT FOR REAGENT AND RESOURCE SHARING

Further information and request for resources and reagents should be directed to and will be fulfilled by the lead contact, Franck Housseau (fhousse1@jhmi.edu).

Il17a$^{-/-}$, *Il17ra*$^{-/-}$, *Il22*$^{-/-}$ and *Il23p19*$^{-/-}$ mice have been provided upon MTA restrictions (see Key Resources Table).

EXPERIMENTAL MODEL AND SUBJECT DETAILS

Mice strains—All mice were maintained under the same specific pathogen-free conditions at an American Association for the Accreditation of Laboratory Animal Care (AAALAC)-accredited animal facility at Johns Hopkins University. All animal housing, breeding and experimental procedures were approved by the Johns Hopkins University Animal Care and Use Committee and conform to regulatory standards.. C57BL/6, CD45.1 C57BL/6, CXCR2$^{-/-}$, CXCR4-FLOX (B6.129P2-*Cxcr4*^{tm2Yzo}/J), CX3CR1$^{gfp/gfp}$ (Cx3cr1^{tm1Litt}), IL6Ra-FLOX (B6;SJL-*Il6ra*$^{tm1.1Drew}$/J), IL6 KO (B6;129S2-*Il6*^{tm1Kopf}/J) mice were purchased from The Jackson Laboratories (Bar Harbor, ME) and Min$^{Apc716/+}$ (*Apc*^{Min}) were obtained from Dr. David Huso (Johns Hopkins University) and bred in the vivarium. STAT3-FLOX (B6.Cg-Stat3^{tm2Aki}) were kindly provided by Dr Chuck Drake (Johns Hopkins University). *Il17a*$^{-/-}$ and *Il17ra*$^{-/-}$ were obtained from Dr Yoichiro Iwakura (Tokyo University of Science, Tokyo, Japan) and Dr Tomas Mustelin (Amgen, Seattle), respectively. *Il23p19*$^{-/-}$ mice and *Il22*$^{-/-}$ mice were kindly provided by Dr N. Ghilardi, and Dr W. Ouyang, respectively (Genentech Inc, San Francisco, CA) and under the condition of an MTA between both institutions. LysM-cre and/or Villin-cre mice were crossed with CXCR4-FLOX (B6.129P2-*Cxcr4*^{tm2Yzo}/J), CX3CR1$^{gfp/gfp}$ (Cx3cr1^{tm1Litt}), IL6Ra-FLOX (B6;SJL-*Il6ra*$^{tm1.1Drew}$/J), STAT3-FLOX (B6.Cg-Stat3^{tm2Aki}) to target selectively myeloid or epithelial cells, respectively, for deletion of the gene of interest. Four-week-old mice on a C57BL/6 background were used for *B fragilis* colonization in all experiments. We previously used male and female mice for ETBF colonization and didn't find any difference. Therefore, each time possible we used female mice, but for complex genetic models, such as conditional KO mice on Min background, we used indifferently male and female mice to accrue enough mice per group. For breeding, two females are generally breed with one male, and resulting litters including KO mice and their control littermates, are co-housed up to 5 mice per cage in all experiments. All mice used in experiments are genotyped according to the protocol provided by the supplier and the conditional KO models were validated by gene expression in the isolated target cells (myeloid or epithelial cells for LysM-CRE or Villin-CRE, respectively).

Bone marrow chimera mice—When conditional KO mice were not available, bone marrow chimera mice were used to test the effect of gene deletion in BM-derived hematopoietic cells versus non-BM derived hematopoietic cells, including epithelial cells. Briefly, 10^7 bone marrow cells from donor mice were injected i.v. into lethally irradiated (1200 cGy; twice 600cG at 4hr interval) 6–8 week-old recipients. BM-reconstituted mice were rested an additional 6 weeks prior to *Bacteroides fragilis* (*B fragilis*) colonization.

***bft-2* isogenic mutant—**ETBF strain 086-54443-2-2 was used to generate a *bft-2* isogenic mutant. This strain harbors two copies of the *bft-2* gene. An in-frame deletion of both *bft-2* gene copies was made using a similar method for creation of *bft-1* mutant (Rhee et al., 2009). In brief, nucleotide fragments flanking the *bft-2* gene were PCR-amplified from stain 086-44443-2-2 using two sets of primers. Primer 1 (BamHI, 5′-TTTACATTGGATCCCATGAGATTGGC) and primer 2 (XhoI, 5′-GGAAGCTGTAACTCGAGTATCAATAGA) amplified 3.06 kb region upstream of *bft-2* and primer 3 (XhoI, 5′-CATGCGGATGCTCGAGAAGATTTGAT and primer 4 (BamHI,

5′-CTAAAAGTTGGATCCGTCCCACTGGA) amplified 3.02 kb down stream of *bft-2* gene (AY372755.1) (Franco et al., 1997). PCR products were inserted into suicide plasmid pGWA34.2(Whittle et al., 2003) by three way ligation to create a plasmid with a truncated *bft-2* gene (pGWA34.2::^bft). pGWA34.2::^bft was introduced into strain 086-54443-2-2 by mating (Rhee et al., 2009; Whittle et al., 2003). The partial *bft-2* mutant (086.17.6) was selected by cefoxitin (20 μg/ml) resistance for single homologous recombination and subsequently by gain of sensitivity to cefoxitin for second homologous recombination. Using forward primer iso7 (5′-GGAGCAGGCAATAACAATCGTCGAC-3′) and reverse primer iso8 (5′-GCATCAGTGGAAATGGGATGAGTAT-3′), we confirmed that the selected clone contained a truncated *bft-2* (0.45 kb) or a full-length (1.2kb) *bft-2* gene. Using the same approach, pGWA34.2::^bft was introduced into the clone with the deletion of the first copy of the *bft-2* gene to delete the second copy of the *bft-2* gene, resulting in the isogenic *bft-2* mutant, 086^bft2.

Bacteria strain growth—Wild type ETBF strain 86-5443-2-2, and isogenic mutant BFT 86-5443-2-2 that does not express BFT [ETBF(*Δbft*)] were used in this study (Wu et al., 2002). Briefly, *B fragilis* strains were grown at 37°C under anaerobic conditions in brain heart infusion (BHI) broth supplemented with hemin (0.5mg/liter), vitamin K_1 (0.1mg/liter), L-cysteine (50mg /liter) and 6 mg/liter of clindamycin was added into brain heart infusion broth for transformed strains (Wick et al., 2014). One colony is grown overnight anaerobically at 37°C and an aliquot is washed in PBS and adjusted to an optical density of 10^9 CFU/ml for mouse inoculations.

Mouse colonization by *B fragilis* strains—As previously described, mice were treated at 4 weeks of age *per os* with antibiotic (clindamycin and streptomycin) for 5 days and then colonized with the *B fragilis* strains (Wu et al., 2009). A 100 μL volume of PBS containing 1×10^8 CFU of *B. fragilis* was administrated by a gavage needle. Antibiotic treatment was stopped after bacterial inoculation. Serial dilution of murine fecal samples were cultured periodically post-inoculation to quantify and monitor continuous ETBF colonization.

Cell line culture—HT29/C1 cells were obtained from Dr. Daniel Louvard (Huet et al., 1987) and used experimentally as previously described (Wu et al., 2007). HT29/C1 cells were grown to 80% confluency in 24 well culture plates in Dulbecco's Modified Eagle Medium (DMEM, 4.5 g/L glucose, L-glutamine, no sodium pyruvate) supplemented with 10% heat-inactivated fetal bovine serum, 100 I.U. penicillin, 100 ug/mL streptomycin. Cells were grown at 37ºC in a cell culture incubator with 10% CO_2.

METHOD DETAILS

Tumor and microadenoma counts—Tumors are counted in formalin-fixed, methylene blue-stained colons blindly by SW and/or CLS. For histologic studies, formalin-fixed tissue was paraffin-embedded (FFPE), sectioned (5μm) and stained with hematoxylin and eosin (H&E staining). Microadenoma were counted by two blinded individuals (DLH and SW).

Pepducin treatment—CXCR2-specific (RTLFKAHMGQKHR) pepducin and negative control (TRFLAKMHQGHKR) peptide were purchased from Genscript (NJ, USA).

Pepducin treatment was performed according to protocols developed by Jamieson et al (Jamieson et al., 2012). In brief, mice received an initial dose of 2.5 mg/kg by subcutaneous injection followed by a daily maintenance dose of 1 mg/kg. Dosing began 24 hours after ETBF infection and continued until harvest.

Leukocyte isolation from gut lamina propria—Proximal and distal colon were cut, washed and enzymatically digested (400 U/ml Liberase and 0.1 mg/ml DNAse1; Roche Diagnostics, Indianapolis, IN) as previously described (Thiele Orberg et al., 2017). Distal colon refers to cell isolation from the smooth, non-ridged, portion of the mouse colon (C1 to C4 in Fig. 2). When cells were isolated from specific segments of the colon, this is labeled in the text. Leukocytes were isolated from single cell suspension using 80/40/20 Percoll density gradient centrifugation (GE Healthcare Life Science, Pittsburgh, PA).

Flow cytometry and cell sorting—Single cell suspensions enriched for leukocytes were characterized according to their myeloid and lymphoid populations by flow cytometry analysis. Myeloid cell staining was performed following the procedure previously described by Thiele-Orberg et al (Thiele Orberg et al., 2017). Briefly, MO-IMC were characterized as $CD45^{+}CD3^{-}CD11b^{hi}Ly6C^{hi}Ly6G^{-}F4/80^{-/low}MHC\text{-}II^{-/low}$, PMN-IMC as $CD45^{+}CD3^{-}CD11b^{hi}$ $Ly6C^{int}Ly6G^{+}F4/80^{-}MHC\text{-}II^{-}$, and Mϕ as $CD45^{+}CD3^{-}CD11b^{int}Ly6C^{-}Ly6G^{-}F4/80^{hi}$ cells. For intracellular cytokine staining, cells were stimulated for 4.5 h with 30 nM phorbol 12-myristate 13-acetate and 1 μM ionomycin (both eBioscience) in presence of Golgistop (BD). Cells were subsequently stained for cell surface markers (CD4-PerCp/Cy5.5, GK1.5; CD3-AF700, 17A2; CD8-PE/CF594, 53-6.7; all Biolegend) followed by fixation/permeabilization (Cytofix/Cytoperm, BD) and staining using IL-17A-Pacific Blue (TC11-18H10.1, Biolegend). Flow cytometry was performed using a LSRII cytometer (BD) and data were analyzed with FACSDiVa 6.1.3 software (BD). For cell sorting experiments, CEC populations were sorted as CD45-EpCAM+ cells using an AriaII cytometer (BD).

Gene expression—RNA was extracted from whole colonic tissue using the RNAeasy kit (Quiagen) and following the manufacturer instructions. Expression of target genes was analyzed using Taqman technology-based pre-designed gene expression kit from ABI (Thermofisher/Life Technologies). For gene expression performed in epithelial cells (Fig. S1), 48 target genes were tested using Taqman technology-based custom-designed PCR array plates (Thermofisher/Life Technologies; Table S1). Expression of the genes of interest was normalized to *Gapdh* expression. Results were expressed as ΔC_t or $\Delta\Delta C_t$ (RQ, relative expression).

Immunohistochemistry—Serial FFPE tissue sections were deparaffinized and antigens retrieved by incubation in citrate buffer before anti-pStat3 staining (Cell Signaling, Danvers, MA) as previously described (Wick et al., 2014). PowerVision HRP mouse anti-rabbit (Leica Microsystems, Bannockburn, IL) was used as secondary. Sections were analyzed on an EcliPSE E800 microscope (Nikon Corporation).

Immunofluorescence—After fixation and paraffin embedding, tissue was cut into 5-μm sections. Antigen retrieval was performed by placing slides containing the sections in a

citrate-based antigen-unmasking solution (Vector Laboratories) and boiling them in a microwave. Following this step, sections were permeabilized for 30 min in 0.2% Triton X-100 in TBS, and blocking of nonspecific reactivity was performed for 45 min in 10%FBS/ 0.2%TritonX-100 in TBS at room temperature (RT). Primary antibodies were diluted in 5% FBS/ 0.2% TritonX-100/ TBS and incubated overnight. Anti-IL-17RA (clone H-168, Rabbit polyclonal, Santa Cruz) was used at a concentration of 1:100. Validation data for this antibody is shown in McAllister et al (McAllister et al., 2014). Slides were then washed three times in 0.2%TritonX-100 in PBS, and sections were incubated with the appropriate fluorescence-conjugated secondary IgG antibodies at a 1:300 dilution for 1 hr at RT in the dark. Alexa 488- conjugated anti-E-cadherin (Mouse IgG2a, BD) antibody was used at a concentration on 1:100. Cy3-conjugated anti-actin alpha-smooth muscle (SMA; SIGMA) was used at 1:750. Nuclei were labeled with DAPI (1:1,000) and slides were mounted in Vectashield mounting medium (Vector Labs). Images were acquired using a Nikon confocal imaging microscope and NIS Elements software.

Isolation of primary colonic epithelial cells for Western Blot analysis—Colonic epithelial cells (CECs) were isolated from mice as previously described (Fu et al., 2016). In brief, after euthanizing mice, the entire colon was removed under aseptic conditions and washed twice with ice-cold PBS. After dividing the colon into 2–3 mm long fragments and transferring them into chelating buffer (27 mM trisodium citrate, 5 mM Na_2HPO_4, 96 mM NaCl, 8 mM KH_2PO_4, 1.5 mM KCl, 0.5 mM DTT, 55 mM D-sorbitol, 44 mM sucrose, 6 mM EDTA, 5 mM EGTA [pH 7.3]) for 15 min at 4°C, CECs were then dislodged by repeated vigorous shaking. Tissue debris was removed by a 40-μm cell-strainer (Fisher Scientific, Suwanee, GA) and CECs were harvested by centrifugation at 4°C. Isolated CECs were cultured at 37°C for 1 h for recovery, followed by indicated treatment. Subcellular fractionation was carried out by differential centrifugation as previously described (Fu et al., 2016).

Immunoblot analysis—Immunoblot assays were conducted as previously described (Fu et al., 2016). Briefly, cells were harvested and lysed on ice by 0.4 ml of lysis buffer (50 mM Tris-HCl [pH 8.0], 150 mM NaCl, 1% NP-40 and 0.5% sodium deoxycholate, 1 × complete protease inhibitor cocktail [Roche Applied Science, Indianapolis, IN]) for 30 min. The lysates were centrifuged at 10,000 × *g* at 4°C for 10 min, and the protein-normalized lysates were subjected to a separation by SDS-PAGE under reduced and denaturing conditions. The resolved protein bands were transferred onto nitrocellulose membranes and probed by the Super Signaling system (Fisher Scientific) according to the manufacturer's instructions, and imaged using a FluorChem E System (Protein Simple, Santa Clara, CA).

IL-8 detection in HT29/C1 cells culture supernatant—HT29/C1 were washed with DMEM and medium was replaced with fresh DMEM for 30 minutes prior to cytokine treatment. BFT, human recombinant IL-17a and TNFα (Thermofisher), were then added for 4hrs. IL-8 was measured in the culture supernatants using ELISA. BD OptEIA Human IL-8 ELISA set (BD Biosciences) was used to coat 96 flat-bottom well Nunc-Immuno polystyrene ELISA plates (Thermofisher) according to manufacturer's specifications. BD Pharmigen TMB substrate reagent (BD Bioscience) was used as the substrate.

ETBF mucosal colonization—Mucosal colonization was confirmed and quantified on approximately 200 μg of tissue collected from the terminal 2 cm of the distal mouse colon and between 1 and 2 cm from the cecum. Tissue was weighed, placed in 500 μl of 0.016% DTT PBS, and vortexed for approximately 10 seconds. Tissue was then rinsed by vortexing twice in saline. Samples were homogenized and quantified (CFU/gm tissue) by plating on selective media as described previously (Boleij et al., 2015).

QUANTIFICATION AND STATISTICAL ANALYSIS

Data were analyzed using Mann-Whitney U test in GraphPad Prism 7. Data are presented as mean ± SEM. p values <0.05 were considered statistically significant.

Supplementary Material

Refer to Web version on PubMed Central for supplementary material.

Acknowledgments

We thank Guillermo Ortega and Dr. Augusto Franco for their contributions to creating the ETBF(*Δbft2*) strain utilized in these studies. Funding for this work was provided by the Bloomberg Philanthropies, National Institutes of Health R01DK080817 (CLS), R01CA151325 (CLS); R01GM111682 (FW); P30DK089502 (GI Center Grant); P30CA006973 (SKCCC core); P50CA062924 (GI SPORE; FH, CLS); K08 DK087856 (ECW).

References

Acharyya S, Oskarsson T, Vanharanta S, Malladi S, Kim J, Morris PG, Manova-Todorova K, Leversha M, Hogg N, Seshan VE, et al. A CXCL1 paracrine network links cancer chemoresistance and metastasis. Cell. 2012; 150:165–178. [PubMed: 22770218]

Boleij A, Hechenbleikner EM, Goodwin AC, Badani R, Stein EM, Lazarev MG, Ellis B, Carroll KC, Albesiano E, Wick EC, et al. The Bacteroides fragilis toxin gene is prevalent in the colon mucosa of colorectal cancer patients. Clin Infect Dis. 2015; 60:208–215. [PubMed: 25305284]

Bollrath J, Phesse TJ, von Burstin VA, Putoczki T, Bennecke M, Bateman T, Nebelsiek T, Lundgren-May T, Canli O, Schwitalla S, et al. gp130-mediated Stat3 activation in enterocytes regulates cell survival and cell-cycle progression during colitis-associated tumorigenesis. Cancer cell. 2009; 15:91–102. [PubMed: 19185844]

Chen K, Eddens T, Trevejo-Nunez G, Way EE, Elsegeiny W, Ricks DM, Garg AV, Erb CJ, Bo M, Wang T, et al. IL-17 Receptor Signaling in the Lung Epithelium Is Required for Mucosal Chemokine Gradients and Pulmonary Host Defense against K. pneumoniae. Cell Host Microbe. 2016; 20:596–605. [PubMed: 27923703]

Conti HR, Bruno VM, Childs EE, Daugherty S, Hunter JP, Mengesha BG, Saevig DL, Hendricks MR, Coleman BM, Brane L, et al. IL-17 Receptor Signaling in Oral Epithelial Cells Is Critical for Protection against Oropharyngeal Candidiasis. Cell Host Microbe. 2016; 20:606–617. [PubMed: 27923704]

De Simone V, Franzè E, Ronchetti G, Colantoni A, Fantini MC, Di Fusco D, Sica GS, Sileri P, MacDonald TT, Pallone F, et al. Th17-type cytokines, IL-6 and TNF-α synergistically activate STAT3 and NF-kB to promote colorectal cancer cell growth. Oncogene. 2015; 34:3493–3503. [PubMed: 25174402]

DeStefano Shields CE, Van Meerbeke SW, Housseau F, Wang H, Huso DL, Casero RA Jr, O'Hagan HM, Sears CL. Reduction of Murine Colon Tumorigenesis Driven by Enterotoxigenic Bacteroides fragilis Using Cefoxitin Treatment. J Infect Dis. 2016; 214:122–129. [PubMed: 26908749]

Franco AA, Mundy LM, Trucksis M, Wu S, Kaper JB, Sears CL. Cloning and characterization of the Bacteroides fragilis metalloprotease toxin gene. Infection and immunity. 1997; 65:1007–1013. [PubMed: 9038310]

Fu K, Sun X, Wier EM, Hodgson A, Liu Y, Sears CL, Wan F. Sam68/KHDRBS1 is critical for colon tumorigenesis by regulating genotoxic stress-induced NF-kappaB activation. Elife. 2016; 5:10. 7554/eLife.15018.

Garg AV, Ahmed M, Vallejo AN, Ma A, Gaffen SL. The deubiquitinase A20 mediates feedback inhibition of interleukin-17 receptor signaling. Sci Signal. 2013; 6:ra44. [PubMed: 23737552]

Grivennikov S, Karin E, Terzic J, Mucida D, Yu GY, Vallabhapurapu S, Scheller J, Rose-John S, Cheroutre H, Eckmann L, et al. IL-6 and Stat3 are required for survival of intestinal epithelial cells and development of colitis-associated cancer. Cancer cell. 2009; 15:103–113. [PubMed: 19185845]

Grivennikov SI, Wang K, Mucida D, Stewart CA, Schnabl B, Jauch D, Taniguchi K, Yu GY, Osterreicher CH, Hung KE, et al. Adenoma-linked barrier defects and microbial products drive IL-23/IL-17-mediated tumour growth. Nature. 2012; 491:254–258. [PubMed: 23034650]

Herjan T, Yao P, Qian W, Li X, Liu C, Bulek K, Sun D, Yang WP, Zhu J, He A, et al. HuR is required for IL-17-induced Act1-mediated CXCL1 and CXCL5 mRNA stabilization. J Immunol. 2013; 191:640–649. [PubMed: 23772036]

Housseau F, Wu S, Wick EC, Fan H, Wu X, Llosa NJ, Smith KN, Tam A, Ganguly S, Wanyiri JW, et al. Redundant Innate and Adaptive Sources of IL17 Production Drive Colon Tumorigenesis. Cancer Res. 2016; 76:2115–2124. [PubMed: 26880802]

Huet C, Sahuquillo-Merino C, Coudrier E, Louvard D. Absorptive and mucus-secreting subclones isolated from a multipotent intestinal cell line (HT-29) provide new models for cell polarity and terminal differentiation. J Cell Biol. 1987; 105:345–357. [PubMed: 3611191]

Iwakura Y, Ishigame H, Saijo S, Nakae S. Functional specialization of interleukin-17 family members. Immunity. 2011; 34:149–162. [PubMed: 21349428]

Jamieson T, Clarke M, Steele CW, Samuel MS, Neumann J, Jung A, Huels D, Olson MF, Das S, Nibbs RJ, et al. Inhibition of CXCR2 profoundly suppresses inflammation-driven and spontaneous tumorigenesis. J Clin Invest. 2012; 122:3127–3144. [PubMed: 22922255]

Kinzler KW, Vogelstein B. Lessons from hereditary colorectal cancer. Cell. 1996; 87:159–170. [PubMed: 8861899]

Kryczek I, Lin Y, Nagarsheth N, Peng D, Zhao L, Zhao E, Vatan L, Szeliga W, Dou Y, Owens S, et al. IL-22(+)CD4(+) T cells promote colorectal cancer stemness via STAT3 transcription factor activation and induction of the methyltransferase DOT1L. Immunity. 2014; 40:772–784. [PubMed: 24816405]

Kumar P, Monin L, Castillo P, Elsegeiny W, Horne W, Eddens T, Vikram A, Good M, Schoenborn AA, Bibby K, et al. Intestinal Interleukin-17 Receptor Signaling Mediates Reciprocal Control of the Gut Microbiota and Autoimmune Inflammation. Immunity. 2016; 44:659–671. [PubMed: 26982366]

Lindemans CA, Calafiore M, Mertelsmann AM, O'Connor MH, Dudakov JA, Jenq RR, Velardi E, Young LF, Smith OM, Lawrence G, et al. Interleukin-22 promotes intestinal-stem-cell-mediated epithelial regeneration. Nature. 2015; 528:560–564. [PubMed: 26649819]

McAllister F, Bailey JM, Alsina J, Nirschl CJ, Sharma R, Fan H, Rattigan Y, Roeser JC, Lankapalli RH, Zhang H, et al. Oncogenic Kras Activates a Hematopoietic-to-Epithelial IL-17 Signaling Axis in Preinvasive Pancreatic Neoplasia. Cancer cell. 2014; 25:621–637. [PubMed: 24823639]

Rhee KJ, Wu S, Wu X, Huso DL, Karim B, Franco AA, Rabizadeh S, Golub JE, Mathews LE, Shin J, et al. Induction of persistent colitis by a human commensal, enterotoxigenic Bacteroides fragilis, in wild-type C57BL/6 mice. Infect Immun. 2009; 77:1708–1718. [PubMed: 19188353]

Sears CL, Garrett WS. Microbes, microbiota, and colon cancer. Cell Host Microbe. 2014; 15:317–328. [PubMed: 24629338]

Thiele Orberg E, Fan H, Tam AJ, Dejea CM, Destefano Shields CE, Wu S, Chung L, Finard BB, Wu X, Fathi P, et al. The myeloid immune signature of enterotoxigenic Bacteroides fragilis-induced murine colon tumorigenesis. Mucosal Immunol. 2017; 10:421–433. [PubMed: 27301879]

Wang K, Kim MK, Di Caro G, Wong J, Shalapour S, Wan J, Zhang W, Zhong Z, Sanchez-Lopez E, Wu LW, et al. Interleukin-17 receptor a signaling in transformed enterocytes promotes early colorectal tumorigenesis. Immunity. 2014; 41:1052–1063. [PubMed: 25526314]

Wang L, Yi T, Kortylewski M, Pardoll DM, Zeng D, Yu H. IL-17 can promote tumor growth through an IL-6-Stat3 signaling pathway. J Exp Med. 2009; 206:1457–1464. [PubMed: 19564351]

Whittle G, Whitehead TR, Hamburger N, Shoemaker NB, Cotta MA, Salyers AA. Identification of a new ribosomal protection type of tetracycline resistance gene, tet(36), from swine manure pits. Appl Environ Microbiol. 2003; 69:4151–4158. [PubMed: 12839793]

Wick EC, Rabizadeh S, Albesiano E, Wu X, Wu S, Chan J, Rhee KJ, Ortega G, Huso DL, Pardoll D, et al. Stat3 activation in murine colitis induced by enterotoxigenic Bacteroides fragilis. Inflamm Bowel Dis. 2014; 20:821–834. [PubMed: 24704822]

Wu S, Dreyfus LA, Tzianabos AO, Hayashi C, Sears CL. Diversity of the metalloprotease toxin produced by enterotoxigenic Bacteroides fragilis. Infection and immunity. 2002; 70:2463–2471. [PubMed: 11953383]

Wu S, Lim KC, Huang J, Saidi RF, Sears CL. Bacteroides fragilis enterotoxin cleaves the zonula adherens protein, E-cadherin. Proceedings of the National Academy of Sciences of the United States of America. 1998; 95:14979–14984. [PubMed: 9844001]

Wu S, Morin PJ, Maouyo D, Sears CL. Bacteroides fragilis enterotoxin induces c-Myc expression and cellular proliferation. Gastroenterology. 2003; 124:392–400. [PubMed: 12557145]

Wu S, Powell J, Mathioudakis N, Kane S, Fernandez E, Sears CL. Bacteroides fragilis enterotoxin induces intestinal epithelial cell secretion of interleukin-8 through mitogen-activated protein kinases and a tyrosine kinase-regulated nuclear factor-kappaB pathway. Infection and immunity. 2004; 72:5832–5839. [PubMed: 15385484]

Wu S, Rhee KJ, Albesiano E, Rabizadeh S, Wu X, Yen HR, Huso DL, Brancati FL, Wick E, McAllister F, et al. A human colonic commensal promotes colon tumorigenesis via activation of T helper type 17 T cell responses. Nat Med. 2009; 15:1016–1022. [PubMed: 19701202]

Wu S, Rhee KJ, Zhang M, Franco A, Sears CL. Bacteroides fragilis toxin stimulates intestinal epithelial cell shedding and gamma-secretase-dependent E-cadherin cleavage. J Cell Sci. 2007; 120:1944–1952. [PubMed: 17504810]

Wu S, Shin J, Zhang G, Cohen M, Franco A, Sears CL. The Bacteroides fragilis toxin binds to a specific intestinal epithelial cell receptor. Infect Immun. 2006; 74:5382–5390. [PubMed: 16926433]

Yu H, Pardoll D, Jove R. STATs in cancer inflammation and immunity: a leading role for STAT3. Nat Rev Cancer. 2009; 9:798–809. [PubMed: 19851315]

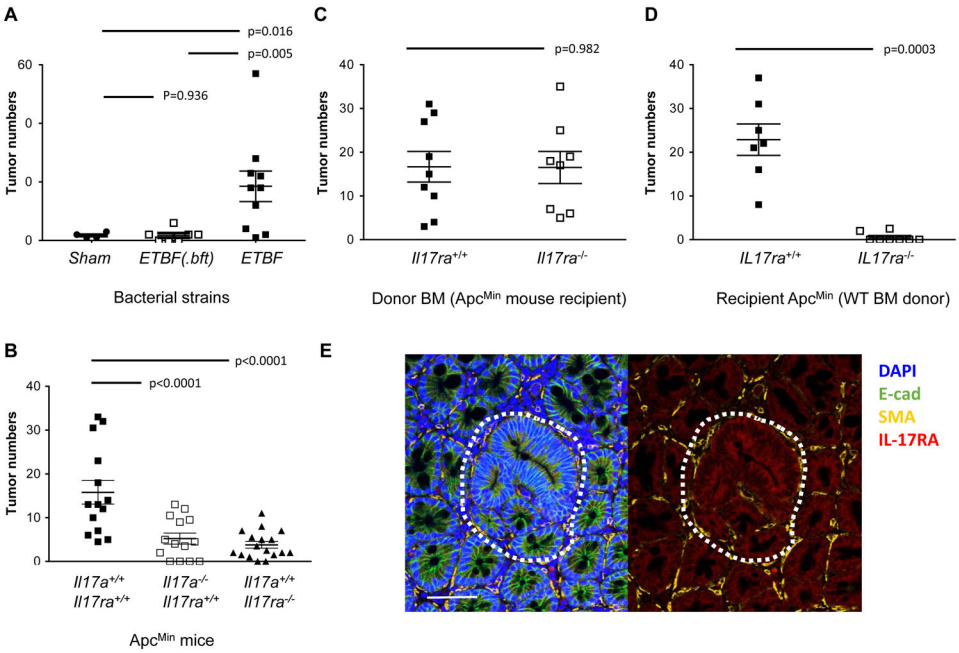

Figure 1. BFT and IL-17 target colonic epithelial cells to promote ETBF-mediated carcinogenesis

A, colon tumor numbers in *Apc*^{Min} mice colonized with ETBF or ETBF(*Δbft*) for a period of 8 weeks. Non-colonized *Apc*^{Min} mice (Sham) were used as control. **B**, colon tumor numbers in parental (Il17a$^{+/+}$Il17ra$^{+/+}$), IL-17A deficient (Il17a$^{-/-}$Il17ra$^{+/+}$) and IL-17RA deficient (Il17a$^{+/+}$Il17ra$^{-/-}$) *Apc*^{Min} mice 12 weeks after ETBF colonization. **C**, colon tumor numbers in [WT(IL17ra$^{+/+}$)> *Apc*^{Min}] and [Il17a$^{-/-}$ C57BL/6 > *Apc*^{Min}] BM chimera mice 12 weeks after ETBF colonization. **D**, colon tumor numbers in [Il17a$^{+/+}$(WT)>*Apc*^{Min}] and [WT>Il17ra$^{-/-}$ *Apc*^{Min}] BM chimera mice 12 weeks after ETBF colonization. Graphs show mean+/− SEM. **E**, Immunofluorescent microscopic analysis of IL-17RA expression in 4 week ETBF-colonized *Apc*^{Min} mice. Blue, DAPI; green, E-cadherin (epithelial cells); yellow, SMA (fibroblasts and myofibroblasts); red, IL-17RA. Dotted line delineates microadenoma. Scale bar, 50 μm

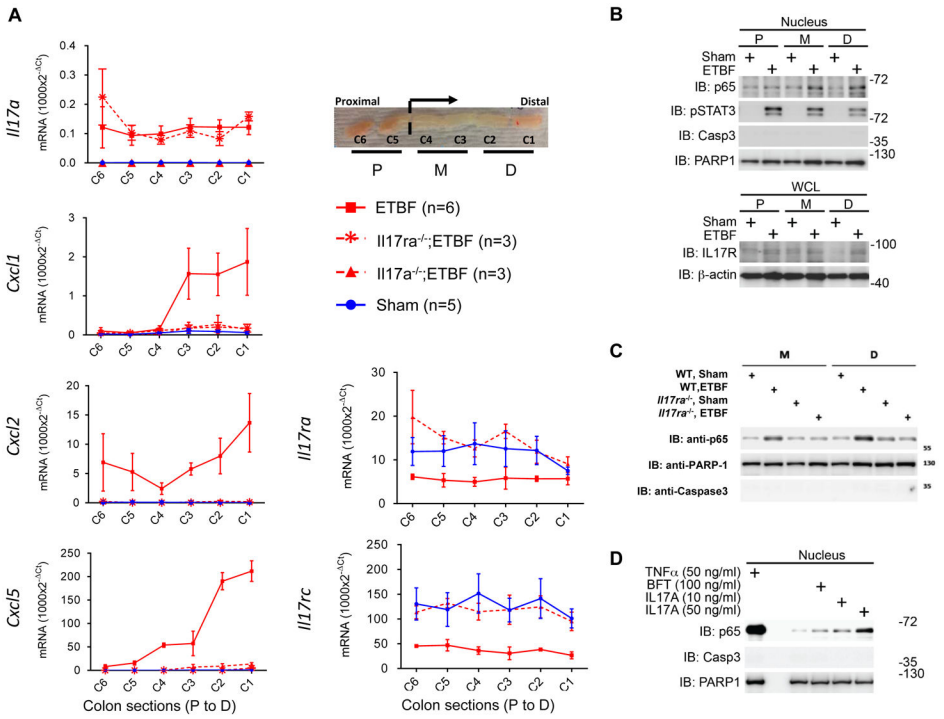

Figure 2. IL-17 dependent NF-κb signaling in CECs triggers higher expression of *Cxcl1*, *Cxcl2* and *Cxcl5* in the distal compared to proximal segments of ETBF-colonized colon

A, *Il17a*, *Il17ra*, *Il17rc*, *Cxcl1*, *Cxcl2* and *Cxcl5* mRNA expression in whole tissue sections from proximal (P; C6) to distal (D; C1) colon of WT (Sham, blue circles; ETBF, red squares), *Il17a*$^{-/-}$ (*Il17a*$^{-/-}$, ETBF, red triangles) and *Il17ra*$^{-/-}$ (*Il17ra*$^{-/-}$, ETBF, red stars) C57BL/6 (WT) mice. A representative image of colon segments C6 to C1 is shown. In panels B–D these segments are grouped into P (C6, C5), M (mid, C4, C3) and D (C2, C1). Ct are normalized with gapdh Ct (ΔCt) and mRNA expression is calculated as $1000x2^{-\Delta Ct}$. **B**, CECs were isolated from proximal (P), mid (M) and distal (D) portions of colons obtained from either Sham or ETBF-colonized C57BL/6 mice at day 7 post infection. *Top*, nuclear fractions derived from the indicated CECs were immunoblotted (IB) for p65 and pStat3. Caspase-3 (Casp3) and PARP1 served as loading controls for cytosolic and nuclear markers, respectively. *Bottom*, whole cell lysates (WCL) derived from the indicated CECs were IB for IL-17R, with β-actin as a loading control. Data are representative of two independent experiments. **C**, CECs were isolated from the mid (M) and distal (D) portions of colons obtained from either Sham or ETBF-colonized *IL-17ra*$^{+/+}$ (WT) or *IL-17ra*$^{-/-}$ C57BL/6 mice at day 7 post-infection. **D**, HT29/c1 cells were stimulated with the indicated concentration of TNFα, purified BFT or IL-17a for 6h. Nuclear fractions were derived and IB for p65. Casp3 and PARP1 served as loading controls and cytosolic and nuclear markers, respectively.

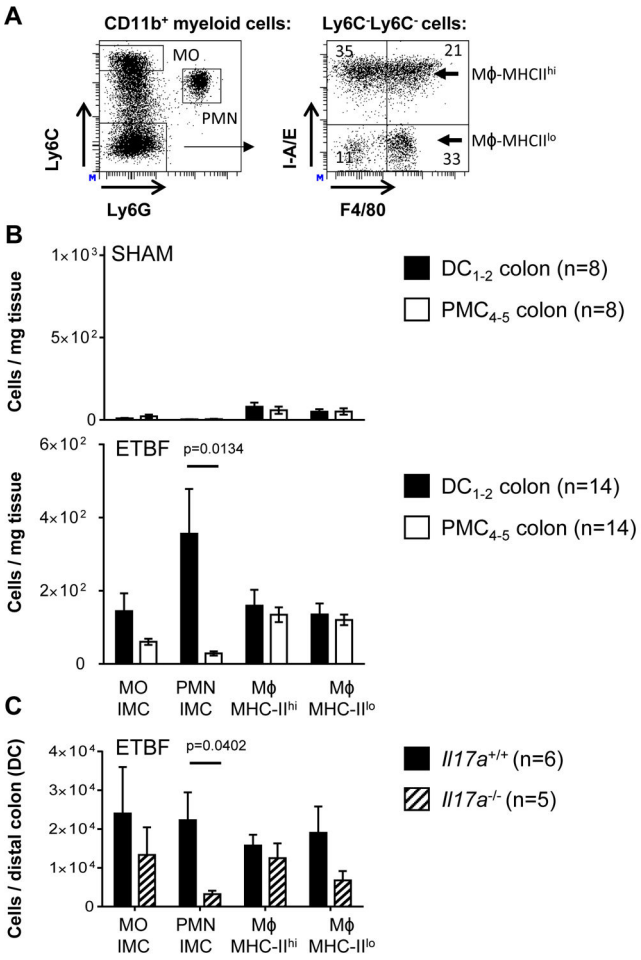

Figure 3. IL-17-dependent accumulation of IMCs in the distal part of the colon upon ETBF colonization of WT mice

A, Gating strategy used to delineate the myeloid population in enzymatically digested colonic LP 7 days after ETBF colonization of WT C57BL/6 mice. MO-IMC and PMN-IMC are defined as $CD45^+CD3^-CD11b^{hi}Ly6C^{hi}Ly6G^-$ and $CD45^+CD3^-CD11b^{hi}Ly6C^{int}Ly6G^+$ respectively. Macrophages (Mϕ) are characterized as $CD45^+CD3^-CD11b^{hi}Ly6C^-Ly6G^-F4/80^+I\text{-}A/E^{hi}$ (Mϕ-MHC-II^{hi}) and $CD45^+CD3^-CD11b^{hi}Ly6C^{-i}Ly6G^-F4/80^+I\text{-}A/E^{lo}$ (Mϕ-MHC-II^{lo}). **B**, Numbers of myeloid cells per mg of tissues in the distal ($DC_{1–2}$, C1–C2) (black bars) and mid-proximal ($PMC_{4–5}$, sections C4–C5, Figure 2) (open bars) colon isolated from Sham C57BL/6 mice (top graph; n=8) and 7 days after ETBF colonization (bottom panel; n=14). % of alive CD45 cells. **C**, Number of myeloid cells in the distal colon (DC) colons isolated from WT (*Il17a*$^{+/+}$; black bars; n=6) and *IL17a*$^{-/-}$ C57BL/6 mice (striped bars; n=5) 7 days after ETBF colonization. % of alive CD45 cells shown. Graphs show mean+/− SEM.

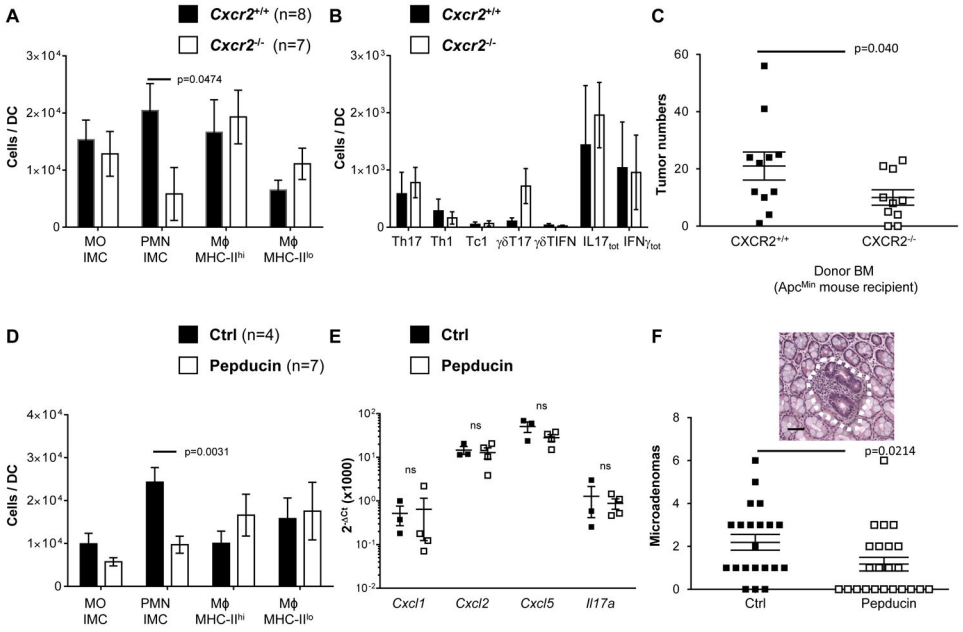

Figure 4. Myeloid recruitment and colon tumorigenesis are impaired upon *Cxcr2* deletion or pepducin-mediated inhibition of CXCR2 in ETBF-colonized *Apc*^{Min} mice

A, Myeloid cell recruitment in the distal colon (DC) of CXCr2$^{+/+}$ WT (black bars; n=8) and CXCR2$^{-/-}$ (open bars; n=7) mice 7 days after ETBF colonization. MO-IMC, CD11b^{+}Ly6C^{hi}Ly6G^{-}F4/80^{-}I-A/Elo; PMN-IMC, CD11b^{+}Ly6C^{lo}Ly6G^{+}F4/80^{-}I-A/E-; Mϕ-MHC-II^{hi}, CD11b^{+}Ly6C^{-}Ly6G^{-}F4/80+I-A/E^{hi}; Mϕ-MHC-II^{lo}, CD11b^{+}Ly6C^{-}Ly6G^{-}F4/80+I-A/Elo. B, Number of IFNγ- and IL-17-producing cells in the distal colon (DC) of CXCr2$^{+/+}$ WT (black bars; n=8) and CXCR2$^{-/-}$ (white bars; n=7) mice 7 days after ETBF colonization. **C**, colon tumor numbers in control [CXCr2$^{+/+}$>*Apc*^{Min}] (n=10) and [CXCr2$^{-/-}$>*Apc*^{Min}] (n=10) BM chimera mice 12 weeks after ETBF colonization. **D**, Myeloid cell recruitment in the distal colon (DC) of WT mice treated with control peptide (ctrl) (black bars; n=4) and the CXCR2 inhibitor pepducin (open bars; n=7) mice 7 days after ETBF colonization. Graphs show mean+/− SEM. **E**, *Il17a, Cxcl1, Cxcl2* and *Cxcl5* gene expression in whole colon tissue (DC$_{1-2}$ portion) of ctrl peptide (black symbols) and the CXCR2 inhibitor pepducin (open symbols)-treated WT mice 7 days after ETBF colonization. Ct are normalized with gapdh Ct (ΔCt) and mRNA expression is calculated as $1000x2^{-\Delta Ct}$. Graphs show mean+/− SEM. **F**, microadenoma numbers in *Apc*^{Min} mice treated with ctrl peptide and the CXCR2 inhibitor pepducin 4 weeks after ETBF colonization. Graphs show mean+/− SEM. A representative micrograph of a colon microadenoma is shown in insert. Scale bar, 50 μm.

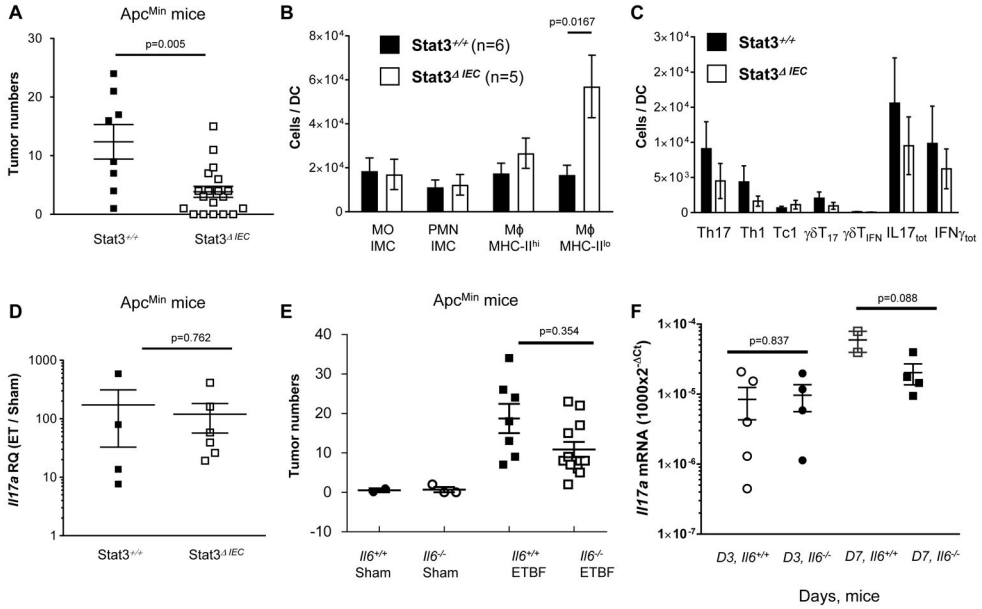

Figure 5. ETBF-triggered colon tumorigenesis in *Apc*^{Min} mice is decreased in absence of epithelial Stat3 signaling

A, colon tumor numbers in Stat3$^{+/+}$ parental (black square; n=8) and Stat3$^{\Delta\ IEC}$(open squares; n=18) *Apc*^{Min} mice 12 weeks after ETBF colonization. **B**, myeloid cell recruitment in the distal colon (DC) of Stat3$^{+/+}$ WT (black bars; n=6) and Stat3$^{\Delta\ IEC}$ (open bars; n=5) mice 7 days after ETBF colonization. MO-IMC, CD11b^{+}Ly6C^{hi}Ly6G^{-}F4/80^{-}I-A/Elo; PMN-IMC, CD11b^{+}Ly6C^{lo}Ly6G^{+}F4/80^{-}I-A/E-; Mϕ-MHC-II^{hi}, CD11b^{+}Ly6C^{-}Ly6G^{-} F4/80^{+} I-A/E^{hi}; Mϕ-MHC-II^{lo}, CD11b^{+}Ly6C^{-}Ly6G^{-} F4/80^{+} I-A/Elo. **C**, Number of IFNγ– and IL-17-producing cells in the distal (DC) colon of Stat3$^{+/+}$ WT (black bars; n=6) and Stat3$^{\Delta\ IEC}$ (white bars; n=5) mice 7 days after ETBF colonization. Graphs show mean+/− SEM. **D**, *Il17a* gene expression in whole colon tissue ($DC_{1–2}$) of IEC$^{Stat3+/+}$ WT (n=4) and IEC$^{Stat3–/–}$ (n=6) mice 7 days after ETBF colonization. Ct are normalized with gapdh Ct (ΔCt). *Il17a* expression is indicated as ratio (RQ) of ΔCt in ETBF mice to ΔCt in Sham mice (ET/Sham). Graphs show mean+/− SEM. **E**, colon tumor numbers in *Il6*$^{+/+}$ parental (Sham, black circle; n=3 and ETBF, black square;n=7) and *Il6*$^{–/–}$ (Sham, open circle; n=4 and ETBF, open square; n=12) *Apc*^{Min} mice 12 weeks after ETBF colonization. Graphs show mean+/− SEM. **F,** *Il17a* gene expression in whole colon tissue of WT (open circle, D3; open square, D7) and *IL6*$^{–/–}$ (black circle, D3; black square, D7) mice 3 and 7 days after ETBF colonization. Ct are normalized with gapdh Ct (ΔCt) and mRNA expression is calculated as $1000x2^{-\Delta Ct}$. Graphs show mean+/− SEM.

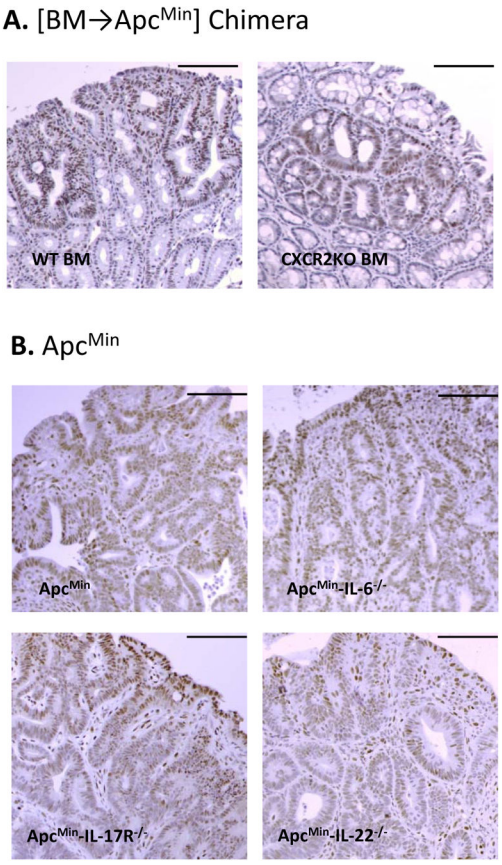

Figure 6. Epithelial Stat3 remains activated in ETBF-colonized *Apc*^{Min} mice in absence of IL-17, IL-6 or CXCR2 expression

A, pStat3 IHC in [CXCr2$^{+/+}$>*Apc*^{Min}] (WT BM; left), [CXCr2$^{-/-}$>*Apc*^{Min}] (CXCR2KO BM; right); **B,** parental *Apc*^{Min} (upper left), *Il6*$^{-/-}$*Apc*^{Min} (upper right), *Il17ra*$^{-/-}$*Apc*^{Min} (bottom left) and Il22$^{-/-}$ *Apc*^{Min}. All mice were sacrificed 12 weeks after ETBF colonization. scale bars, 100um.

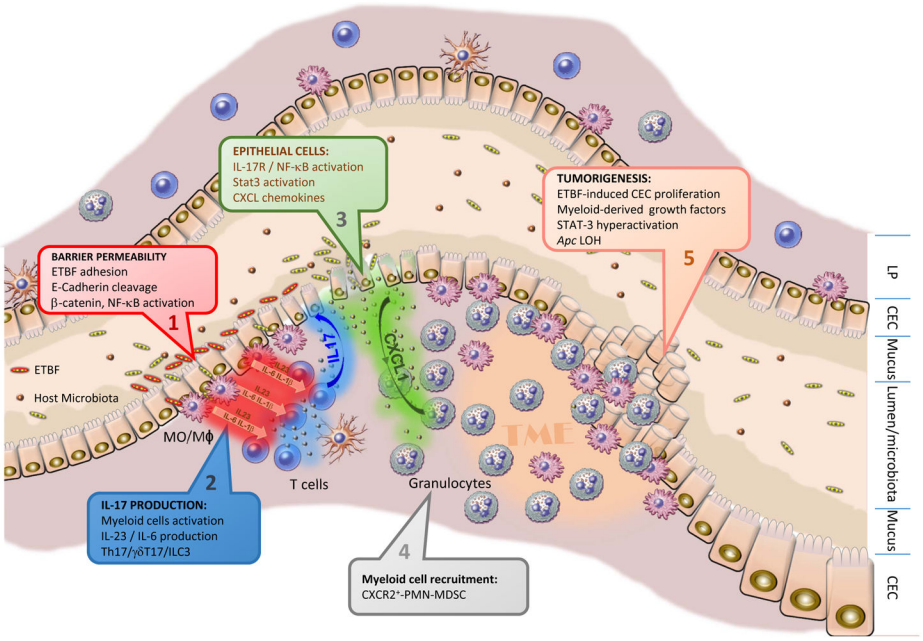

Figure 7. Schematic representation of the mechanistic CEC:mucosal relay promoting ETBF-induced colon tumorigenesis

Collectively the data herein support a model whereby ETBF infection triggers a specific relay of cellular interactions initiated by the action of the single bacterial virulence protein, BFT, on CECs that results first in IL-17-producing mucosal immune cells that then turn to act on the CECs to initiate a NFκB-associated CEC immune response that directs distal colon myeloid mucosal infiltration key to ETBF tumor localization in the distal colon. ETBF orchestrated colon carcinogenesis occurs in the absence of IL-6 and IL-23. CEC Stat3 activation is a necessary, but not sufficient, complement to the actions of IL-17. Steps in this model include: **1,** ETBF produces BFT, a zinc-metalloprotease that induces E-cadherin cleavage that contributes to barrier permeability dysfunction as well as Wnt/βcatenin and NF-κB signaling pathway activation. **2**, a diminished colonic mucosal barrier likely contributes to resident myeloid cells activation that contributes to the rapid onset ETBF IL-17 signature characterized by the accumulation of Th17, γδT17 and ILC3. Further, dependent on redundant cytokines due to the BFT virulence protein of ETBF, Stat3 is highly activated in lamina propia ICs including lymphocytes and myeloid cells. **3**, IL-17/IL-17R and BFT signaling pathways converge on CECs to activate a distal colon NF-κB cascade resulting in the production of a C-X-C chemokine distal colon mucosal gradient, including CXCL1 (homologous to human IL-8). **4**, although the ETBF-altered colon barrier progressively recovers its integrity, ETBF persistence maintains IL-17 production and the chemokine gradient that promotes the accumulation of distal colon MDSCs, including high proportions of PMN-MDSC. **5**, the oncogenic properties of BFT including BFT-induced CEC proliferation and DNA damage likely allow the rapid loss of the second *Apc* allele (loss of heterozygosity, LOH) and rapid promotion of microadenoma formation (DeStefano Shields et al., 2016; Wu et al., 2003). MDSC accumulation in the distal colon provides growth factors promoting adenoma growth.

KEY RESOURCES TABLE

REAGENT or RESOURCE	SOURCE	IDENTIFIER
Antibodies		
BD Horizon™ V500 Rat Anti-Mouse CD45	BD Biosciences	Cat# 561487; RRID:AB_10697046
PerCP/Cy5.5 anti-mouse/human CD11b [M1/70]	BioLegend	Cat# 101228; RRID:AB_893232
Pacific Blue™ anti-mouse Ly-6C [HK1.4]	BioLegend	Cat# 128013; RRID:AB_1732090
Alexa Fluor® 647 anti-mouse Ly-6G [1A8]	BioLegend	Cat# 127610; RRID:AB_1134159
Alexa Fluor® 488 anti-mouse I-A/I-E [M5/114.15.2]	BioLegend	Cat# 107616; RRID:AB_493523
Alexa Fluor® 700 anti-mouse CD86 [GL-1]	BioLegend	Cat# 105023; RRID:AB_493720
BD Pharmingen™ APC-Cy™7 Hamster Anti-Mouse CD11c [HL3]	Thermo Fisher	Cat# 561241
Anti-Mouse CD103 (Integrin alpha E) PE	Thermo Fisher	Cat# 12-1031-81; RRID:AB_465798
PE/Cy7 anti-mouse F4/80 [BM8]	BioLegend	Cat# 123113; RRID:AB_893490
Pacific Blue™ anti-mouse CD45.2	BioLegend	Cat# 109819; RRID:AB_492873
PerCP/Cy5.5 anti-mouse CD8a [53-6.7]	BioLegend	Cat# 100734 RRID:AB_2075238
BD Pharmingen™ PE-Cy™7 Rat Anti-Mouse CD90.2	DB Biosciences	Cat# 561642; RRID:AB_10895975
BD Horizon™ PE-CF594 Rat Anti-Mouse CD4 [RM4–5]	DB Biosciences	Cat# 562285; RRID:AB_11154410
BD Horizon™ BV786 Hamster Anti-mouse CD3 [145-2C11]	DB Biosciences	Cat# 564379
BD Horizon™ BV711 Hamster Anti-Mouse γδ T-Cell Receptor [GL3]	DB Biosciences	Cat# 563994
BV605 Rat Anti-Mouse CD335 (NKp46) [29A1.4]	DB Biosciences	Cat# 564069
Anti-Mouse/Rat Foxp3 Alexa Fluor® 488 [FJK-16s]	Thermo fisher	Cat# 53-5773-82; RRID:AB_763537
Alexa Fluor® 700 anti-mouse IL-17A [TC11-18H10.1]	BioLegend	Cat# 506914; RRID:AB_536016
Brilliant Violet 510™ anti-mouse IFN-γ [XMG1.2]	DB Biosciences	Cat# 505841
PE anti mouse EpCam [G8.8]	DB Biosciences	Cat# 563477
Phospho-Stat3 (Tyr705) [D3A7] XP® Rabbit mAb	Cell Signaling technology	Cat#9145S; RRID:AB_2491009
IL-17RA [H-168]	Santa-Cruz	Cat# sc-30175; RRID:AB_2125539
AF-488 E-cadherin [36/E]	BD Biosciences	Cat# 560061; RRID:AB_1645347
Cy3-conjugated anti-actin alpha-smooth muscle [1A4]	SIGMA-Aldrich	Cat# C6198; RRID:AB_476856
P65 [C-20]	Santa-Cruz	Cat#sc-372-G; RRID:AB_632037
Casp3 western blot	Cell Signaling technology	Cat# 9662S RRID:AB_10694681
Parp1 [46D11] western blot	Cell Signaling technology	Cat# 9532 RRID:AB_659884
IL17RA [LS-B6868]	LifeSpan	Cat# LS-B6868-50 RRID:AB_11186527

REAGENT or RESOURCE	SOURCE	IDENTIFIER
Beta actin [AC-15] western blot	Sigma-Aldrich	Cat# A5441 RRID:AB_476744
Bacterial and Virus Strains		
ETBF strain 86-5443-2-2	Wu et al, 2002	NA
ETBF(Δ*bft2*) isogenic strain	Wu et al, 2002	NA
Biological Samples		
Chemicals, Peptides, and Recombinant Proteins		
CXCR2-specific pepducin peptide (RTLFKAHMGQKHR)	Genscript	N/A
Pepducin ctrl peptide (TRFLAKMHQGHKR)	Genscript	N/A
Liberase TM	Sigma Aldrich	Cat#5401127001
DNAse1	Sigma Aldrich	Cat#10104159001
Recombinant human TNFa	R&D System	Cat#210-TA
Recombinant human IL-17A	Thermo Fisher	Cat#14-8179-62
Critical Commercial Assays		
fixation/permeabilization	BD Bioscience	Cat#554714
High capacity RNA to CDNA kit	Thermo Fisher	Cat#4387406
Taqman Master mix	Thermo Fisher	Cat#4444557
Taqman pre amp master mix	Thermo Fisher	Cat#4488593
RNAeasy micro kit	Quiagen	Cat#74004
OptEIA Human IL-8 set	BD Bioscience	Cat#555244
Deposited Data		
Experimental Models: Cell Lines		
HT29/C1	Dr Daniel Louvard (Institut Pasteur, Paris)	NA
Experimental Models: Organisms/Strains		
C57BL/6J	The Jackson Lab	RRID:IMSR_JAX:000664
CD45.1 C57BL/6 B6.SJL-*Ptprc*^{a} *Pepc*^{b}/BoyJ	The Jackson Lab	RRID:IMSR_JAX:002014
Min$^{ApcΔ716+/-}$ (Min) mice	Dr B. Vogelstein (Johns Hopkins Univ)	N/A
Cxcr2 KO B6.129S2(C)-*Cxcr2*^{tm1Mwm}/J	The Jackson Lab	RRID:IMSR_JAX:006848
Cxcr4-FLOX (B6.129P2-Cxcr4^{tm2Yzo}/J)	The Jackson Lab	RRID:IMSR_JAX:008767
Cx3cr1 gfp/gfp (Cx3cr1^{tm1Litt})	The Jackson Lab	RRID:IMSR_JAX:005582
Il6ra-FLOX (B6;SJL-il6ra$^{tm1.1Drew}$/J)	The Jackson Lab	RRID:IMSR_JAX:012944
Il6$^{-/-}$ (B6;129S2-il6tm1Kopf/J)	The Jackson Lab	RRID:IMSR_JAX:002650
Lyzm-CRE (B6.129P2-Lyz2$^{tm1(cre)Ifo}$/J)	The Jackson Lab	RRID:IMSR_JAX:004781
Villin-CRE (B6.Cg-Tg(Vil1-Cre)997Gum/J	The Jackson Lab	RRID:IMSR_JAX:004586
Il23p19$^{-/-}$	N Ghilardi (Genentech, San Francisco))	NA
Il22$^{-/-}$	W. Ouyang (Genentech, San Francisco)	NA
Stat3-FLOX (B6.Cg-Stat3^{tm2Aki})	C Drake (JHU)	NA
Il17a−/−	Y Iwakura (Tokyo university of Science)	NA

REAGENT or RESOURCE	SOURCE	IDENTIFIER
Il17ra$^{-/-}$	T Mustelin (Amgen, Seattle)	NA
Oligonucleotides		
Primer shown in Table S1	Thermo Fisher	Cat#4331182
Recombinant DNA		
Software and Algorithms		
FACSDiVa 6.1.3	http://www.bdbiosciences.com/instruments/software/facsdiva/index.jsp	BD FACSDiva Software, RRID:SCR_001456
Prism	http://www.graphpad.com/	Graphpad Prism, RRID:SCR_002798
NIS Elements software (immunofluorescence)	https://www.nikoninstruments.com/Products/Software	NIS-Elements, RRID:SCR_014329
Other		
Purified BFT	Wu et al, 2002	N/A